EXAMENSARBETE INOM TEKNIK,
GRUNDNIVÅ, 15 HP
STOCKHOLM, SVERIGE 2020

A novel chitosan-stearic coating with bee-pollen microcapsules for corrosion protection

ALBIN ANDERSSON

KTH
SKOLAN FÖR INDUSTRIELL TEKNIK OCH MANAGEMENT

ABSTRACT

In this project a novel chitosan-stearic acid (CS-SA) coating with bee-pollen microcapsules for encapsulation of 2-mecraptobenzothiazole (MBT) as a waterborne formulation for a biocompatible corrosion protection coating was developed and the coating properties was analyzed. Hydrophobic stearic acid (SA) was crosslinked with via a carbodiimide reaction to form micelles and is assembled on the bee-pollen grains and the chitosan matrix was further self-crosslinked using glutaraldehyde (GA). Stearic acid was used to hydrophobically interact with modified pollen and with further crosslinking with the chitosan, which was proven successful by FTIR results. The encapsulation of anticorrosive agent MBT into pollen was successful and examined by UV-Vis spectroscopy, however, the pollen cannot form a fully stable formulation with the chitosan micelle matrix, partially due to its relatively big size (ca. 20 µm), causing problems with forming a proper barrier protection. The size of the grains and the interference of the carbodiimide crosslinking is the most severe problems with the pollen microcapsules. Therefore, no further testing of the corrosive properties could be done, which requires a dense and stable coating to sustain in salty water for the whole measurement period. As the reference coatings without pollen provided much more promising results, especially when crosslinked with GA, the conclusion is that the reactivity of the pollen is proven difficult to crosslink, and choosing a proper size of a microcontainer and the appropriate encapsulation method in the binder matrix is vital and important for developing a corrosion protective coating.

SAMMANFATTNING

Detta projekt bygger på framställningen och analysen av en tidigare outforskad chitosan-stearinsyra (CS-SA) färg med bi pollen som mikrokapslar för inkapsling av 2-mercaptobenzothiazole (MBT) som en vattenlöslig och biokompatibel anti-korrosions färg. CS-SA var tillverkat med en carbodiimide reaktion för att bilda miceller som ska omslutna pollenkornen, och även ett försök med vidare tvärbindning mellan chitosanen med glutaraldehyde (GA) gjordes. Stearinsyra fick interagera hydrofobiskt med den modifierade pollen och tvärbindes sedan med chitosan, som visade sig vara lyckad med hjälp av FTIR analys. Enkapsuleringen av MBT visade sig med UV-Vis spektroskopi vara lyckad, dock på grund av pollens stora korn (ca 20 µm) orsakade problem med att bilda en stabil barriär mot omgivningen. Storleken av pollen och dess reaktivitet med carbodiimide tvärbindningen är de mest alvarliga problemen med pollen som mikrokapslar, och därav gjordes inga vidare tester av korrosions egenskaperna då detta kräver en täckande och stabil film genom hela mätningen. Då även referensfärgen som gjordes utan pollen gav avsevärt mycket bättre resultat i det avseendet är slutsatsen att reaktiviteten av pollen gör det problematiskt att tvärbinda med chitosan och valet av en kapsel av rätt storlek och hur den inkapslar är avgörande för att utveckla en bra korrosions skyddande färg.

PREFACE

I would like to thank the Unit of Functional materials at the Dept. of material- and nanophysics at KTH to have given me the opportunity to work along them on this project along with giving me a professional insight in now the work of a researcher looks.

Special thanks go to Professor Joydeep Duta for taking me in and Doctor Fei Ye for being my supervisor, along with the rest of the of the members of the unit to have helped me along the way.

Appreciation should also go to Alessandro Armani who worked besides me on a different approach of the same bigger project I worked on, who were a great resource to bounce ideas and thoughts with.

Unfortunately, due to the events with Covid-19 taking place around the globe at the time of the project, most of the property analysis tests that were planned could not take place due to a lockdown on the lab and a change of course to a slightly reduced project were had to be made.

Finally, I would like to thank my wonderful family who have given me a lot of love and support during the course of the project.

Albin Andersson
7th June 2020, Saltsjö-boo

List of abbreviations and acronyms

MBT	2-Mercaptobenzothiazole
CS-SA	Chitosan-steric acid
GA	Glutaraldehyde
GlcNAc	N-acetyl-D-glucosamine
GlcN	Glucosamine
DDA	Degree of acetylation
DS	Degree of substitution
OA	oleic acid
EE	Encapsulation Efficiency
LC	Loading Capacity
EDC	1-Ethyl-3-(3-dimethylaminopropyl)carbodiimide
NHS	N-hydroxysuccinimide
UV-Vis	Ultraviolet-visible spectroscopy
AcOH	Acetic acid
FTIR	Fourier-transformation infrared
FTIR-ATR	Fourier-transformation infrared – Attuned Total Reflection
NaOH	Sodium hydroxide
DCM	Dichloromethane
THF	tetrahydrofuran

TABLE OF CONTENT

1 INTRODUCTION

1.1 PURPOSE

In recent years an increase of toxic waste in oceans have been noted which cause devastating damage on the aquatic life such as fish and coral reefs, and an effort to reduce these emission have been a focus of the industry as well as in research [1]. A common application that cause toxic waste is coatings used for protecting metallic surfaces in aqueous environments which during its lifetime release their additives such as heavy metals or volatile organic compounds, which initially was added to enhance their properties [2]. These additives are generally more commonly than not toxic and not biocompatible and therefore the need for biocompatible and non-toxic coatings have been a hot topic in research as of late. Chitosan derivatives are a prominent candidate for such coatings due to its inherent biocompatible, film-forming ability, anti-microbial activity along with intrinsic self-healing properties to provide an excellent passive corrosion protection [3]. Further improvements on the anti-corrosive properties can be achieved by loading anti-corrosion agents such as 2-Mercaptobenzothiazole (MBT) to provide an active protection for when the passive protection won't be enough such as when the coating has been damaged [4]. Unfortunately, these molecules have the tendency to be released when they are not needed, and hence the incorporation of encapsulating these agents to provide a smart release have been studied with good results in epoxy matrices inter alti [5].

1.2 GOAL

This project aims to create a formulation and evaluate the efficiency of using a Chitosan-Stearic acid (CS-SA) derivative with pollen microcapsules to achieve a smart release of the encapsulated anti-corrosion agent to be used as a biocompatible and environmentally friendly coating. The CS-SA will form micelles in aqueous environments with a hydrophobic core [6] to encapsulate the MBT inside. As the MBT is well soluble in water, it will first be put inside treated bee-pollen to allow the MBT to be encapsulated into the micelles. When treated, the pollens core will be cleaned out to allow other chemicals to be encapsulated [7,8] which will be used to allow the MBT to be encapsulated inside the micelles. To further ensure the encapsulation of the pollen, the stearic acid will be attached to the surface of the pollen grains prior to crosslinking with chitosan to enhance the immobilization of the pollen and MBT. Further investigation to see if self-crosslinking the chitosan to itself using glutaraldehyde (GA) will further improve the properties will be done as well.

The goal is to create a formulation that will provide a coating that will encapsulate the MBT in the pollen into the chitosan matrix to provide a good corrosive protection along with having self-healing properties. The aim is for the coating to be used without any too advanced equipment or procedure to allow it to be used by the mean man. A focus is made on the formulation of the coating and the surface structure along the properties of the coating.

2 BASAL CONCEPTS

Although this project has a more of a practical approach, some more advanced theoretical concepts will be presented in this chapter to allow the reader to comprehend the basics of the coating more thoroughly. Concepts such as the functions of the main components in the coatings, the chemical and physical mechanics that are used as well as a overview of how the analyze methods works will be presented in this chapter.

2.1 COMPONENTS

2.1.1 Chitosan

Chitosan is a linear polysaccharide consisting of blocks of N-acetyl-D-glucosamine (GlcNAc) and glucosamine (GlcN) that is derived from deacetylation of chitin, which is after cellulose the most abundant natural amino polysaccharide on the planet with an approximated minimum $1.1 * 10^{13}$kg present in the biosphere [9]. The most common source of chitin is the exoskeleton of crustaceans which consist of up to $70W_{\%}$ chitin. Deacetylation is the process of removing the acetyl group of the GlcNAc and replacing it with an amine group to form GlcN.

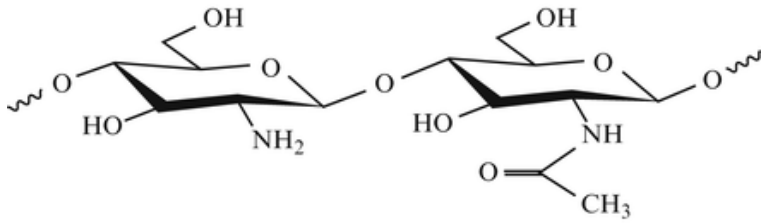

Fig 1, Chemical structure of chitosan showing a deacetylated group (GlcN) to the left, and a non-deacetylated group (GlcNAc) to the right [9].

Chitosan is widely researched due to its many desirable properties such as self-healing, anti-microbial, biocompatibility, biodegradability among others, and provide much futuristic potential due to its reactive amino and hydroxyl groups. These groups give the possibility to modify the chitosan's physicochemical properties and makes chitosan a very versatile molecule [9, 10].

The Molecular weight ($\mathrm{M_w}$) and the degree of deacetylation (DDA) are two properties that greatly affect many chitosan's properties, for instance the anti-microbial activity of chitosan is directly proportional to the DDA and increases with higher $\mathrm{M_w}$ and hence it is ofttimes desirable to have a high DDA. Commercial chitosan generally lies in the range of 40-98% DDA and a M_w between 50 000 and 200 000. The DDA of chitosan is defined as the fraction of amine groups over the total amount of amine and acetyl side groups and can be formulated as

$$DDA = 100 * \frac{n_{GlcN}}{n_{GlcN} + n_{GlcNAc}} . \quad (1)$$

A high DDA reduces the degradation rate of the chitosan allowing films of chitosan to last for months in acidic environments [10].

The chitosan derivative to be used in this project is chitosan-stearic acid (CS-SA), where the carboxylic group of the stearic acid will be attached to the amine group on the chitosan. This will make the long

hydrocarbon chain of the stearic acid to act as hydrophobic while the chitosan will be hydrophilic due to its $\beta(1\rightarrow4)$ linked D-glucosamine structure [11] which will allow the CS-SA to form micelles of the size around 30-130nm when in a aqueous environment [12]. These micelles have proven to have an increased encapsulation effect, smaller micelle size and a more stable colloidal system with a higher degree of substitution (DS) of the amine groups on the chitosan [12, 13]. For micelles to form in a solution, a critical micelle concentration and critical micelle temperature must be reached [14].

2.1.2 2-Mercaptobenzothiazole

2-Mercapltobenzithiazole (MBT) is an organosulfur compound consisting of a benzene ring fused to a 2-mercaptothiazole ring and is generally used in vulcanization of rubber [15]. It is also one of the most efficient and versatile corrosion inhibitors for protecting copper, carbon steel and among other alloys [3,4]. The high electron density of the nitrogen and sulfur on the MBT will make it act as an absorption centers for the metal and may form self-assembled monolayers [16]. These monolayers are by chemisorption attached to the metal surface by the sulfur groups while the rest of the MBT form a highly ordered, packed and hydrophobic layer against the environment to prevent solution to reach the metal to start a corrosive reaction [17, 18]. The application of MBT straight into a metal protective coating have proven to reduce their quantity and efficiency [16] and thus the incorporation of nanocontainers to encapsulate them is a widely used practice for using MBT as an inhibitor [16, 19]. The nanocontainers will make the MBT immobile and thereby only be released when certain criteria are met, such as a certain pH or NaCl concentration [16, 19].

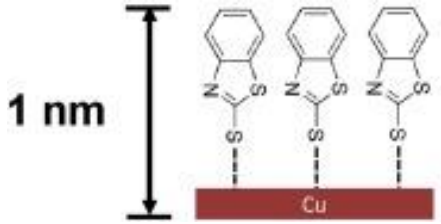

Fig 2. Illustration of formed monolayers of MBT on copper [20].

2.1.3 Pollen

Pollen has for some time been of interest as a biobased microcontainer for applications such as drug delivery and lithium-ion batteries [7, 21]. The pollen shell consists of the exine, a highly porous layer consisting of mainly sporopollenin and the intine, an inner layer consisting of mainly cellulose. Inside the shell resides the cytoplasm which consists of vitamins, proteins, and other materials relevant to the biological functions of the pollen. When the cytoplasm is removed it allow the remaining pollen shell to act as a microcontainer for loading chemicals into [7, 8], and is commonly removed by treating the pollen in alcohol which will penetrate the shell and dissolve the substances [21]. The sporopollenin on the surface of the pollen shell can be cleaned using supersonic treatment in an alcohol solution [21] to allow it to thereafter be further treated using organic compounds to change the pollens properties, such as making it attach to toxic heavy metals for cleaning water or changing its solubility in certain medias to provide a more stable system [22, 23].

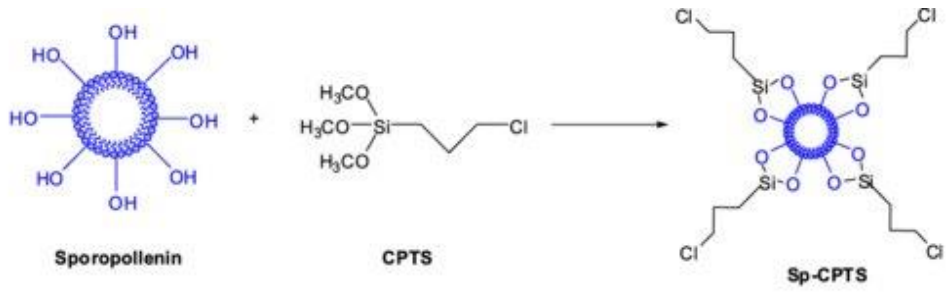

Fig 3, possible sporopollenin surface structure and surface modification [24].

2.2 COATING PROPERTIES

2.2.1 Corrosive properties

Coatings used to prevent corrosion of metallic surfaces can be categorized into three groups based on their functionality; barrier, inhibitive and sacrificial, which are often combined to provide a more efficient corrosion protective coating [25].

The barrier coatings prevent the surrounding environment to be in contact with the metallic surface in the form of creating a passive non-porous layer. If the layer is penetrated the corrosive protection will be lost, and its lifespan is thereby enhanced by an increased thickness of the film.

The inhibitive coatings have substrate that react with the metal along the corrosive atmosphere when the film is penetrated, to inhibit the corrosion reaction. As the substrate is spent whenever it comes in contact with the atmosphere the protective effect is reduced over time. Red lead is a traditional example of an inhibitive coating [25,26].

The sacrificial coatings act as an additive that corrodes instead of the protected metallic surface and will be effective even though the layer has been damaged. The protective effect is based on the additive content amount in the coating. A very common example of a sacrificial coating is galvanized steel [25,26].

2.2.2 Viscosity

The viscosity of a coating gives an idea on how easily it will be applied to a surface, the coverage of the coating and whether the paint tents to spatter if applied by spraying. A rule of thumb used in the coating industry is that viscosity of around 100cP is desirable despite if it applied by a brush, spray, or roll. Measurement of the viscosity can although be a little tricky, as depending on the type of application it should be measured with a method using an appropriate shear stress as the liquid can be non-Newtonian. For spray painting the shear stresses often lies around 1000 to 40,000 s^{-1} when applied with air in contrast to the viscosity for using a brush for the paint which lies around 60s^{-1} [27].

2.2.3 Hydrophobicity

Water molecules have a relatively high surface tension due to it is an electrical dipole, which will result in it wetting surfaces that has a relatively low surface energy such as glass and form beads on surfaces with

a higher surface energy such as Teflon [28]. The classical way to determine if a surface is hydrophobic is to see it the contact angle of the droplet is >90°. An alternative approach would be to look at the double layer and the zeta-potential. The double layer is a structure formed on a surface while in contact with a different phase, forming two parallel layers of charged layers by the interaction of the ions present in the system [29]. The size of this layer is determined by the surface potential as a result of these ion interactions and in turn grow larger with an increased surface potential, making it harder for particles to penetrate this boundary [29]. As the presence of a double layer is relative to the surface tension [30], a hydrophobic coating will prevent the diffusion of water molecules and in turn reduce the corrosive effect on the surface below.

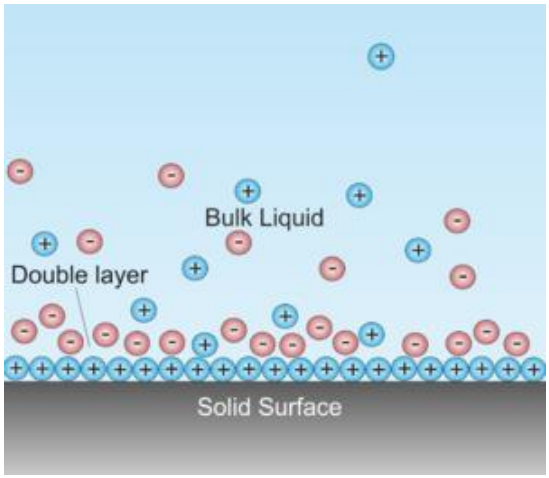

Fig 4, Illustration of a double layer [31]

There are also applications of hydrophilic coatings for windows. The water will spread out more evenly on the surface which will reduce optical scattering from the otherwise beads formed on the surface, which in turn will increase the visibility of the windows [32].

2.2.4 Self-healing properties

Self-healing materials has the property for it to repair itself when damaged and are abundant in biological systems such as living tissues, although man-made polymers have been presented in ever increasing numbers [33]. Self-healing materials can be classified as being either extrinsic or intrinsic, where extrinsic self-healing materials have a healing agent encapsulated into the matrix that are released upon damage to repair the broken matrix. One example is the encapsulation of a catalysts into a polymer bulk what when cracked will be released and start a new polymerization reaction to rebuild the bulk polymer [34]. Intrinsic self-healing materials on the other hand has a molecular structure of the matrix that provide the healing properties. There are generally two different mechanics for intrinsic self-healing materials based on either non-covalent reactions or dynamic covalent reactions. The former is based on physically crosslinked systems and utilize crystallization, ionic/electrostatic interactions, hydrogen bonds or hydrophobic interactions while the latter utilize enzyme-induced crosslinked bonds, Diels-Alder cycloaddition, oxime bonds, Schiff base formations among others [33,35].

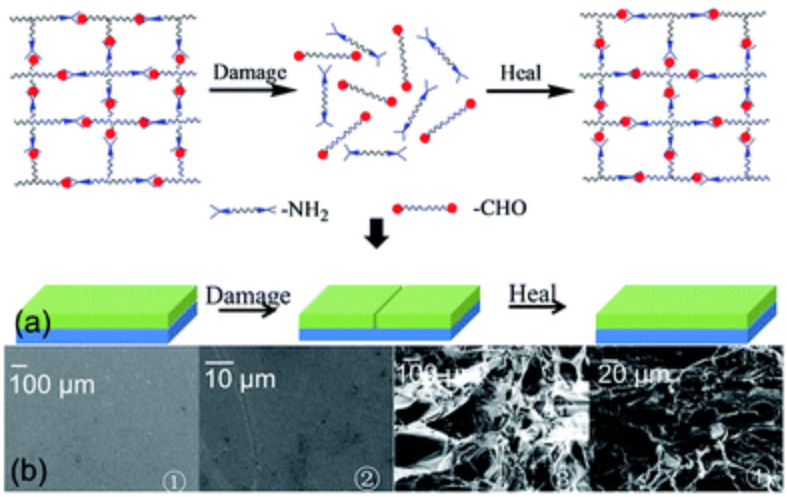

Fig 5, Schematics and SEM images at different magnifications of the dynamic self-healing process using Schiff base linkage. The material is a chitosan and poly(ethylene glycol) functionalized via dialdehyde groups derivative [36].

2.3 ENCAPSULATION

Encapsulation is the process of encapsulating an active substance inside a matrix to protect them against the environment while providing a release of the substance under certain desired conditions [37]. It is commonly used in pharmaceutical, food and cosmetic industries to make the encapsulated substance release over a longer time or be protected from certain environments to avoid chemical reactions or degradation of the active substance [38]. Encapsulated molecules have been of great interest in the coating industry to be incorporated into coatings to provide a smart release, to only be released when a certain criteria such as pH or fracture to the coating has occurred, to provide corrosion protection or self-healing properties [39,40,41,42,43].

A capsule consists of two parts, the core which consists of the encapsulated active substance and the shell which can be in the form of a solid, liquid or gas bubbles whose structures are widely varied [37]. In a general sense there are two different kinds of encapsulations methods; chemical techniques which can either be based on coacervation, co-crystallization or molecular inclusion, and physical techniques which can be freeze drying, extrusion, spray cooling among others. The size of the capsule is generally either in the nano or microscale, where a smaller size provides more efficient encapsulation of the substance [37]. The release of the core material can be either controlled and based on degradation of the shell by melting, destruction, or erosion, or it can be uncontrolled and based on leakage, barrier release, diffusion, or pressure activation. To achieve a controlled release of the core material is a critical step in creating an encapsulated material as it will provide with a more efficient usage of the core material, and to no be release when its undesirable [37].

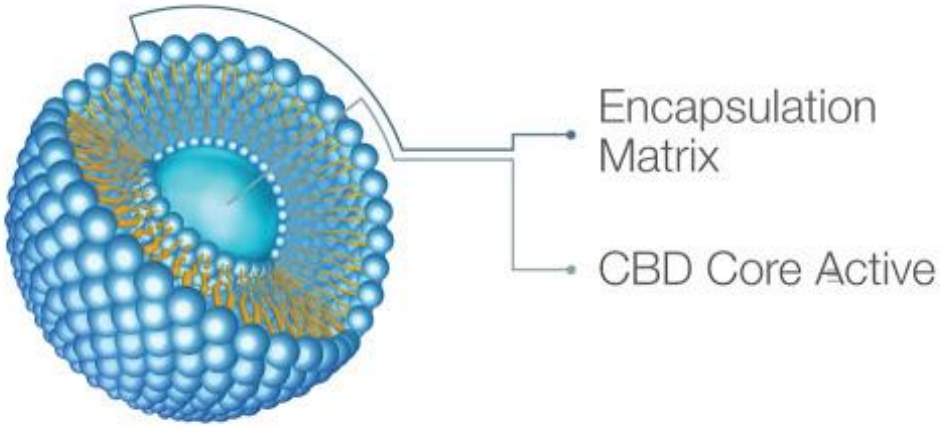

Fig 6, Illustration of a nanocontainer used for encapsulation of CBD oil [44].

Two common measurements on how well an encapsulation is Encapsulation Efficiency (EE) and Loading Capacity (LC). EE is the quota of successfully entrapped substance over the total substance added during the formulation, while LC is the amount of successfully entrapped substance per unit weight of the particles that the core consists of [45].

2.4 CROSSLINKING CHEMISTRY

Crosslinking is the process of creating a network structure out of multiple polymer chains to create a more rigid system and immobile system. The crosslinks can be categorized as either physical or chemical, where the former is based on physically crosslinked systems and utilize crystallization, ionic/electrostatic interactions, hydrogen bonds or hydrophobic interactions while the latter utilize enzyme-induced crosslinked bonds, Diels-Alder cycloaddition, oxime bonds, Schiff base formations among others [33,35]. The chemical crosslinking is achieved by letting the different reactive groups reach thermodynamic equilibrium and form a new bond with a lower energy than before for instance when glutaraldehyde (GA) and chitosan's primary amine together forms imide bonds [46]. Crosslinkers are though often needed to be used as a stepping board in linking two groups together, which is a molecule with two functional groups on either end [47]. The reactive group of the crosslinker are its most important aspect and establishes the method and mechanism for the chemical modification and most commonly include primary amides, sulfhydryl's, carbonyls, carbohydrates and carboxylic acids functional groups [47].

One of the most common crosslinkers for creating amide bonds out of carboxylates and primary amides are 1-Ethyl-3-(3-dimethylaminopropyl)carbodiimide (EDC) which is a zero-length crosslinker, meaning the two functional groups are bound directly to each other without any extra new carbon chain between them is formed [47]. The EDC first bind to the carboxylic group to form an active intermediate that is prone to nucleophilic attack from primary amides to complete the conjugation, se figure below. The rest product is a water-soluble urea derivative and the EDC reaction is as most effective at slight acidic conditions. N-hydroxysuccinimide (NHS) are a common crosslinker to be used together with EDC to increase its efficiency by crosslinking the NHS to the carboxyl to form an NHS ester that's more stable than the

intermediate formed from the EDC alone. NHS esters are most efficient in a slight alkaline condition and creates rest products in the form of NHS [47].

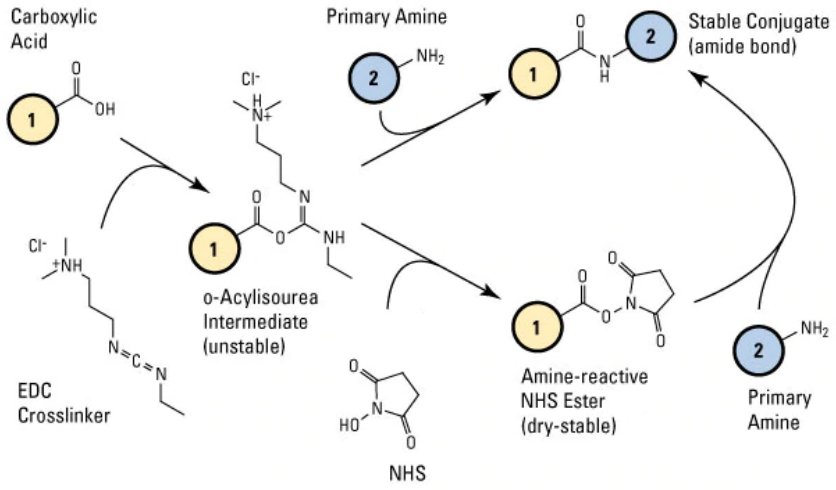

Fig 7, schematic reaction of NHS/EDC crosslinking of a carboxyl and a primary amine to form an amide bond [47]. The upper path of is without the NHS reaction taking place.

2.5 ANALYZE METHODS

2.5.1 UV-vis spectroscopy

Ultraviolet-visible spectroscopy (UV-vis) is a common method to analyze chemical structures where the absorption of electromagnetic radiation around the 190-750nm range and the following excitation of electrons to higher energy states are of interest. For organic molecules it is the functional groups of the molecule known as chromophores that are absorbed due to their low excitation energy in their valence electrons [48]. Many functional groups have a linear relation of their absorbance to their concentration, although some needs to be analyzed for their first, second or even third derivatives, as the bandwidth of the peaks decreases with higher order or derivative [49], and also are often less subjected to background noise [50].

UV-Vis can be used on liquid, solid as well as gaseous phases where solutions and crystals are generally analyzed by transmission, and powdered samples analyzed in diffuse reflection mode known as Diffuse Reflectance Spectroscopy (DRS). The process uses Beer-lambert law, which relates the absorption of electromagnetic waves passing through the material to its properties

$$A = \epsilon bc \tag{2}$$

where A is the absorption, ϵ the molar absorptivity ($m^2 mol^{-1}$), b the path length through the material and c is the molar concentration [51].

While analyzing chitosan derivates using UV-Vis it is common to analyze it in acetic acid (AcOH) in a 1.0cm quartz cell at ambient conditions due to the crystal's and the solutions absence of absorptivity at the relevant wavelengths. The absorbance of GlcNAc monomer of Chitosan have shown to have a linear relation to its concentration in its first derivative to at 199nm in the range of 0.5 – 5.0 mg/l [50, 52].

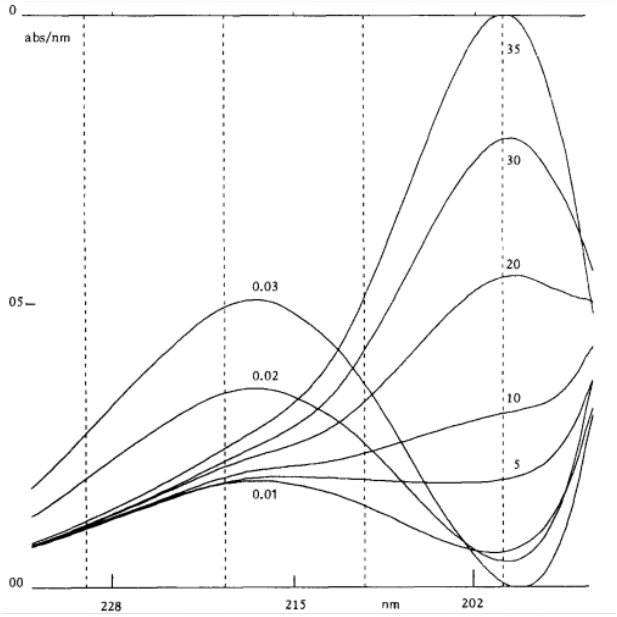

Fig 8, First derivative spectra of 0.01, 0.02 and 0.03 M AcOH and for GlcNAc at concentrations of 5 to 35 mg/l in 0.01 M AcOH [52].

2.5.2 FTIR spectroscopy

Fourier-transformation infrared (FTIR) spectroscopy is used to obtain the infrared spectrum of absorption and reflection of liquid, gas, and solid phases in a high resolution. Unlike UV-VIS that react to functional groups on the molecules, the wavelength absorbed in the infrared spectrum react to the bonds and configurations of polymers giving them a unique fingerprint. The bonds can either stretch or bend when in the presence of infrared radiation, where the bond will change its bond distance or its bond angle respectively. These changes will absorb energy of a specific wavelength and therefore less radiation will be transmitted. The energies needed to bend or stretch different bonds are more or less unique, making the identification of which bonds are present in the material analyzed to be done using databases of known bond energies [53].

An accessory often used with FTIR is the Attuned Total Reflection (FTIR-ATR) that is used to analyze surface structure instead of the bulk of the material. The FTIR-ATR analyzes the changes of the internal IR beam as it comes in contact with the sample. The IR beam is sent through a crystal often made of Germanium or Zinc Selenide which has a high refractive index which will evanescent the beam as it comes into contact with the sample where it will be attenuated to be returned through the crystal and be analyzed. FTIR-ATR is often preferred as it required minimal sample preparation, it's easy to clean and its efficiency at analyzing thick or strongly absorbing samples [54].

3 EXPERIMENT/METHOD

3.1 PREPARATION OF COMPONENTS

3.1.1 Deacetylation of chitosan

As a high DDA of the chitosan is important to achieve a good derivative, the quality of the commercial powder used will be tested as well as trying to improve the DDA of the chitosan using the following method:

3.5g chitosan powder from Sigma-Aldrich was dispersed in diluted 70ml distilled water with 40% sodium hydroxide (NaOH) in a measurement cup and stirred for 3-5min. When the chitosan was completely dispersed, the content was put into an Autoclave set at 140^0C, 0.11MPa for 120 min. The result was washed by distilled water by filtration until it reached a neutral pH and thereafter put in an oven at 105^0C until completely dry.

To create a calibration curve to evaluate the DDA, GlcNAc of concentrations of 0.005, 0.010, 0.015, 0.020, 0.025, 0.030, 0.035, 0.04 mg/ml in AcOH was prepared and analyzed in a Perkin Elmer's Lambda 750 UV/VIS spectrophotometer for their first derivatives. Treated and untreated chitosan of concentration of 1mg/ml acetic acid was then prepared and analyzed and compared to the calibration curve.

3.1.2 Pollen-oleic acid

To make the pollen into a microcontainer the cytoplasm must be removed from its core before treating it with oleic acid (OA) to form a more stable organic phase for the pollen.

Bee-pollen from Bulk Powders is dispersed 5% w/v in ethanol and stirred for 30 minutes using ultrasound and thereafter centrifuged for 10 minutes at 10000rpm. The ethanol is decanted and dispersed in ethanol in a new beaker. The solution was again stirred using ultrasound and centrifuged. The pollen was poured into a 1:1 ethanol and formaldehyde solution and stirred for 10 minutes. The solution is centrifuged and decanted and the pollen is thereafter dried in a vacuum oven at 0.15 bar for 12h at 40°C.

The pollen was dispersed in OA at 0.2g /ml. 70 mL of water were poured in a round flask, partially immersed in an oil bath. The flask was connected to a tubular condenser with water in and water out. When the temperature reached 110°C, pollen in OA solution was poured drop-by-drop in the water in the flask while stirred for 2h and thereafter centrifuged and washed with ethanol twice.

3.2 FORMULATION OF CHITOSAN-STEARIC ACID COATING

3.2.1 chitosan-stearic acid crosslinking

25mg chitosan was dispersed in 1.5ml AcOH and 34mg SA was dispersed in 3.5ml ethanol separately under constant mixing at ambient conditions. 9.5mg EDC was added to the SA solution and left to react for an hour under constant mixing. 34mg NHS was added to the SA solution under constant mixing. NaOH was added to the chitosan solution under constant mixing to change its pH to close to 6 and thereafter added

to the SA solution and left to react under constant mixing for an hour. NaOH was added to the solution until the pH were above 9 and precipitated the CS-SA polymer. The CS-SA solution was washed thrice by centrifugation at 10000rpm for 10min before being decanted and dispersed in first NaHCO3, distilled water and lastly 0.2% AcOH to remove any unreacted stearic acid. The solute was lyophilized using liquid nitrogen and then grinded to achieve a fine powder. The powder was analyzed using FTIR-ATR spectroscopy.

3.2.2 Loading pollen into chitosan-stearic acid

Three different iterations were made:

- Loading pollen-OA into previously made CS-SA micelles
- Binding the SA onto the surface to pollen prior to crosslinking to increase stabilization of the micelles
- Decreasing the Degree of substitution (DS) of the amines from 50% to 25%

Iteration 1 - adding pollen into formed micelles

50mg pollen-OA were suspended in 1ml CH2Cl2 under sonication. 50mg CS-SA dissolved in 5 ml 0.2% AcOH was added to 15ml water. Under vigorous stirring the pollen were dropwise added to the solution and then sonicated to disperse the pollen. The solution was stirring until the CH2Cl2 had evaporated and thereafter centrifuged at 5000rpm for 10min to remove the un-encapsulated pollen using decantation.

Iteration 2 – 50% DS

40mg pollen-OA were dispersed in 8ml dichloromethane (DCM) and thereafter added to 85mg SA dispersed in 8.5ml ethanol under stirring and left to react for 1h. The solution was centrifuged at 10000 rpm for 10min and then decanted and dispersed in ethanol to remove any unreacted SA. 46mg EDC were dispersed in 1 ml ethanol and added to the SA-pollen mixture and left to react for 1h under stirring. 173mg NHS were dispersed in 1ml ethanol and added to the SA-pollen mixture. 125mg chitosan were dispersed in 6.3ml AcOH and NaOH were dropwise added to increase the pH to improve the react ability of NHS. The chitosan solution was thereafter added to the SA-pollen and left to react for 1h.

Iteration 3 – 25% DS

40mg pollen-OA were dispersed in 8ml DCM and thereafter added to 46mg SA dispersed in 4.25ml ethanol under stirring and left to react for 1h. The solution was centrifuged at 10000 rpm for 10min and then decanted and dispersed in ethanol to remove any unreacted SA. 23mg EDC were dispersed in 1 ml ethanol and added to the SA-pollen mixture and left to react for 1h under stirring. 84mg NHS were dispersed in 1ml ethanol and added to the SA-pollen mixture. 125mg chitosan were dispersed in 6.3ml AcOH and NaOH were dropwise added to increase the pH to improve the react ability of NHS. The chitosan solution was thereafter added to the SA-pollen and left to react for 1h.

3.2.3 Loading 2-mercatzobenzothiazole into pollen and chitosan-stearic acid

12.5mg pollen-OA were dispersed in 2.5ml DCM and thereafter added to 42.5mg SA dispersed in 4.5ml ethanol under stirring and left to react for 1h. 2.5mg MBT dispersed in 0.5ml ethanol were added and left

to react for 1h. The solution was centrifuged at 10000rpm for 10minutes, decanted and dispersed in tetrahydrofuran (THF) to remove any unloaded MBT and unreacted stearic acid. 23mg EDC were dispersed in 1 ml ethanol and added to the SA-pollen mixture and left to react for 1h under stirring. 85mg NHS were dispersed in 1ml ethanol and added to the SA-pollen mixture. 125mg chitosan were dispersed in 6.3ml 1% AcOH and NaOH were dropwise added to increase the pH to improve the react ability of NHS. The chitosan solution was thereafter added to the SA-pollen and left to react for 1h.

The solution was diluted down to 1:20, 1:40, 1:60 and 1:80 and analyzed using UV/VIV at 320nm to be compared to a calibration curve to determine the amount of MBT loaded into the system. The calibration curve was made by analyzing MBT dissolved in ethanol at 0.02, 0.015, 0.01, 0.005 and 0.002 mg/ml at 320nm.

3.3 ANALYZATION OF SURFACE PROPERTIES

The final formulation was repeated for 25%, 50% and 100% DS of amine groups on the chitosan to SA using the formulation from 3.23, but with altered proportions of the SA, EDC, and NHS. Further crosslinking using the 50% DS formulation was used to crosslink the amine groups of the chitosan to itself using 4%, 7% and 10% GA to chitosan weight ratio as well as the 25% DS was further crosslinked using 7% GA. The same amount of pollen and MBT was loaded into the coatings. Reference coatings without any pollen or MBT loaded into it was also made to see the difference pollen makes. A total of 11 different iterations was analyzed that will be referred to as: 25DS, 50DS, 100DS, 25DS-7GA, 50DS-4GA, 50DS-7GA, 50DS-10GA, 25DS-X, 50DS-X, 100DS-X, 25DS-7GA-X, where 25DS-7GA refers to the coating with 25% DS and 7% GA and the X iterations are 25DS, 50DS, 100DS and 25DS-7GA without any pollen loaded into them.

GA crosslinking

2ml of the 50DS coating was added to 3 separate beakers, and 2ml of the 25DS coating was added to another beaker, and the amount of chitosan in it was calculated. 25% GA aqueous solution was added to the solutions in relative proportions to add up to 4/7/10% weight to chitosan in the 50DS solutions, and 7% in the 25DS solution, and was stirred for 1 hour.

Application on stainless-steel plates

The coatings were applied dropwise using a pipette onto stainless-steel plates that had been polished to a mirrorlike surface and left to dry. Multiple layers of the coating were applied to achieve a proper thickness. The thicknesses of the coatings were analyzed using a gauge meter, the surface distribution of the pollen particles was analyzed under microscope, and the contact angle of water on the coating surfaces was analyzed.

3.4 FTIR OF ISOLATED REACTIONS

To get a more thorough understanding if any unwanted reactions are taking place under the formulation, FTIR-ATR spectroscopy of isolated reactions are analyzed. The samples were prepared in a similar fashion as they were added during the formulation.

Pollen-OA + SA

Pollen-OA and SA was dispersed in ethanol in separate beakers. When dissolved completely the pollen-OA solution was poured into the SA solution and left to react for 1h. The solution was washed by centrifugation at 10000rpm for 10min before being applied to a polished stainless-steel plate to be analyzed with the FTIR.

Pollen-SA + MBT

Pollen-SA and SMBT was dispersed in ethanol in separate beakers. When dissolved completely the MBT solution was poured into the pollen-SA solution and left to react for 1h. The solution was washed by centrifugation at 10000rpm for 10min before being applied to a polished stainless-steel plate to be analyzed with the FTIR.

25% DS CS-SA + GA

25% DS CS-SA polymer was formulated in the same fashion as 3.2.3. GA solution was added to the polymer at a rate of 7% of the chitosan weight and left to react for 1 hour. The solution was applied to a polished stainless-steel plate to be analyzed with the FTIR.

Pollen-OA + CS

Pollen-OA was dispersed in ethanol and EDC was added to it and left to react for 1h. NHS was added to the solution and left to react for 15min. Chitosan was dissolved in 2% AcOH and added to the pollen-OA and left to react for 1h. The solution was applied to a polished stainless-steel plate to be analyzed with the FTIR.

Pollen-OA + MBT

Pollen-OA was dispersed in ethanol and MBT was added to the solution and left to react for 1h. The solution was washed by centrifugation at 10000rpm for 10min before being applied to a polished stainless-steel plate to be analyzed with the FTIR.

Pollen + GA

Pollen-OA was dispersed in ethanol and GA was added to the solution and left to react for 1h. The solution was washed by centrifugation at 10000rpm for 10min before being applied to a polished stainless-steel plate to be analyzed with the FTIR.

3.5 SUBMERSION TEST

To get an understanding as to how stable the coatings are when in an aqueous environment for a prolonged time, the coatings was submerged in water for up to 24h and then picked up to let try. The coatings analyzed were the ones made under 3.3.

4 RESULTS

4.1 DEACETYLATION OF CHITOSAN

The DDA of commercial chitosan was calculated to 88.5%, while the DDA of treated chitosan was calculated to 90.5% which was derived from Fig 9-10.

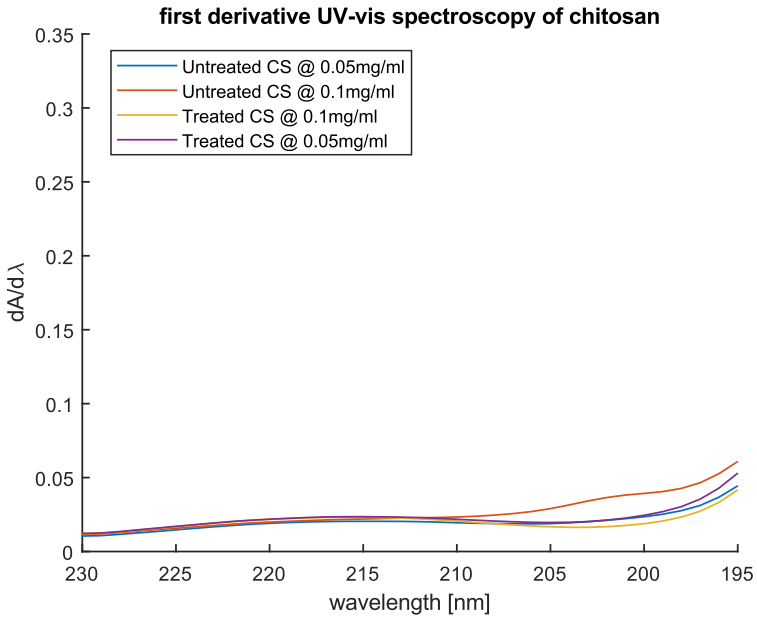

Fig 9, first derivative UV-vis spectroscopy of treated and untreated chitosan at different concentrations in acetic acid.

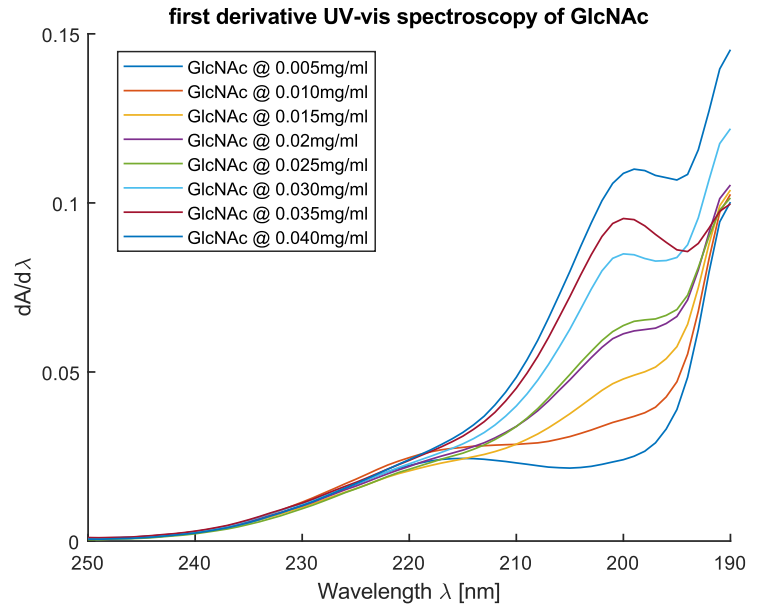

Fig 10a, first derivative UV-vis spectroscopy of GlcNAc at different concentrations in acetic acid.

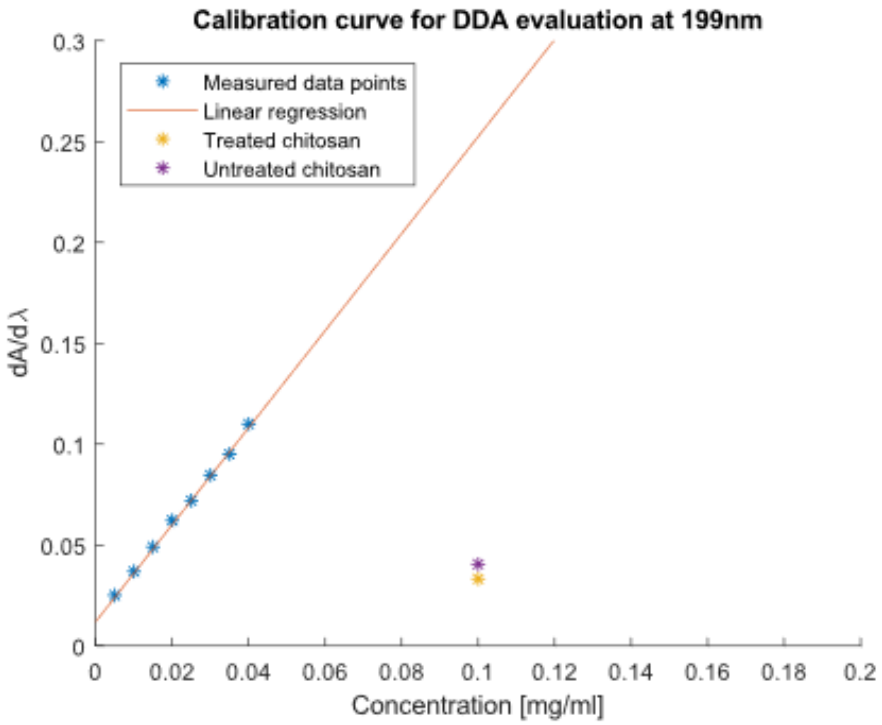

Fig 10b, Calibration curve for DDA evaluation

4.2 FORMULATION OF CHITOSAN-STEARIC ACID COATING

In fig 11 the results of the analysis of the CS and SA crosslinking using the EDC/NHS reaction is presented.

4.2.1 chitosan-stearic acid crosslinking

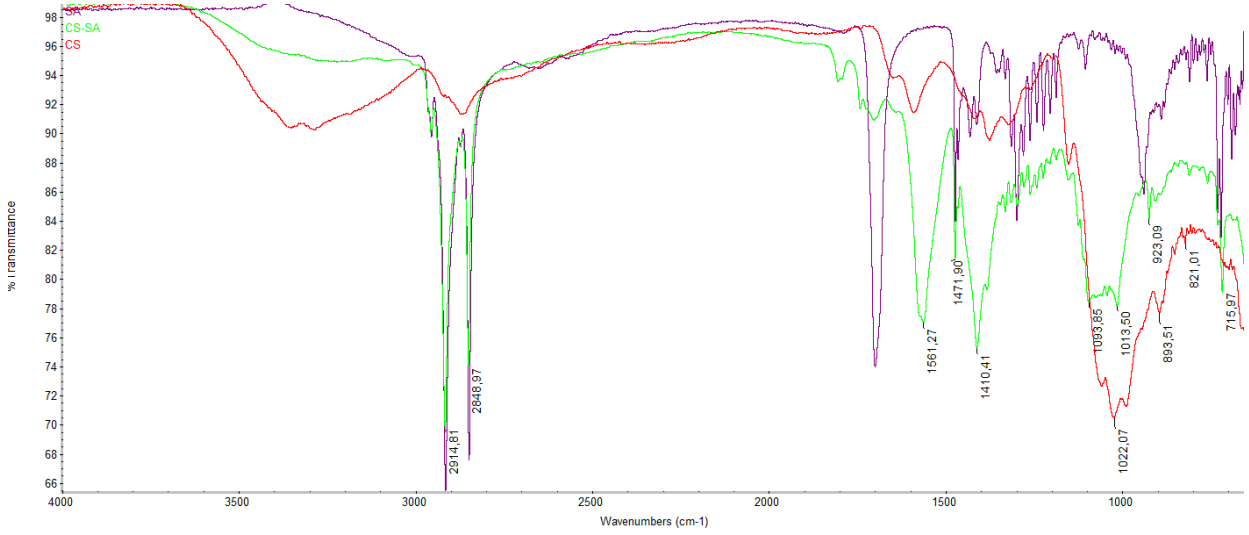

Fig 11, FTIR-ATR spectroscopy of chitosan powder (red), stearic acid powder (purple) and CS-SA powder (green).

4.2.2 Loading pollen into chitosan-stearic acid

Iteration 1 – adding pollen into formed micelles

Brown particles was seen precipitated on the bottom almost instantly after stirring.

Iteration 2- 50% DS, pollen added forming micelles

A homogeneous solution was formed which were opaque and foamy. After a few hours, a small amount of brownish slurry had precipitated to the bottom.

Iteration 3 – 25% DS, pollen added forming micelles

A homogeneous solution was formed which were clear and without foam. After a few hours, a small amount of brownish slurry had precipitated to the bottom.

4.2.3 Loading 2-mercatzobenzothiazole into pollen and chitosan-stearic acid

The results of the evaluation of the amount of encapsulated MBT in the coating is shown in fig 12 and presented in table 1. The creation of the calibration curve that was used to calculate the values in table 1 is presented in fig 13a and 13b.

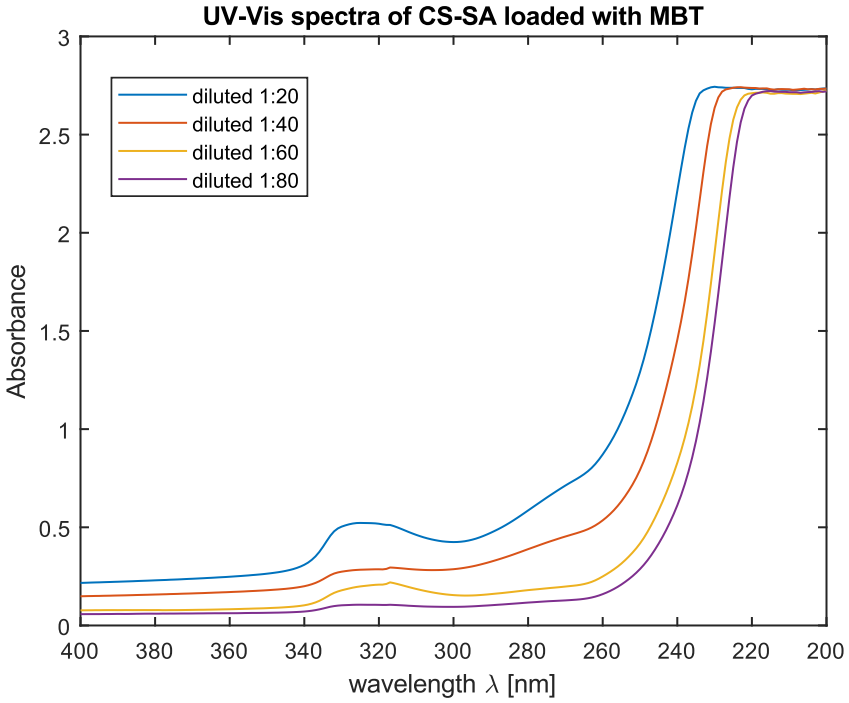

Fig 12, UV-vis spectra of the CS-SA loaded with MBT diluted to different concentrations in ethanol, showing the peak of MBT at 320nm.

Table 1, Loading capacity evaluation of MBT in CS-SA with pollen.

Concentration	1:20	1:40	1:60	1:80
Absorption	0.94320	0.49478	0.41564	0.28040
Amount MBT [mg]	0.8687	0.8786	1.0906	0.9361
Loading capacity	0.69%	0.70%	0.87%	0.75%

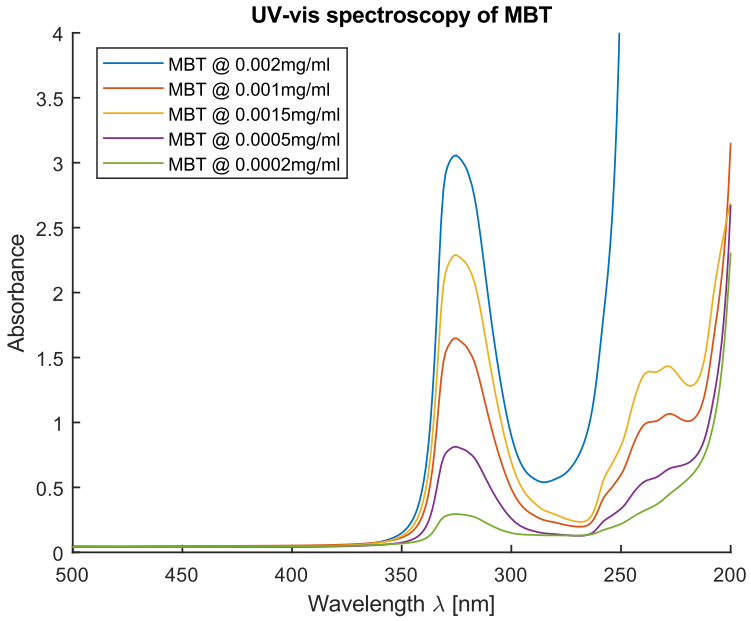

Fig 13a, UV-vis spectroscopy of MBT at different concentrations in ethanol

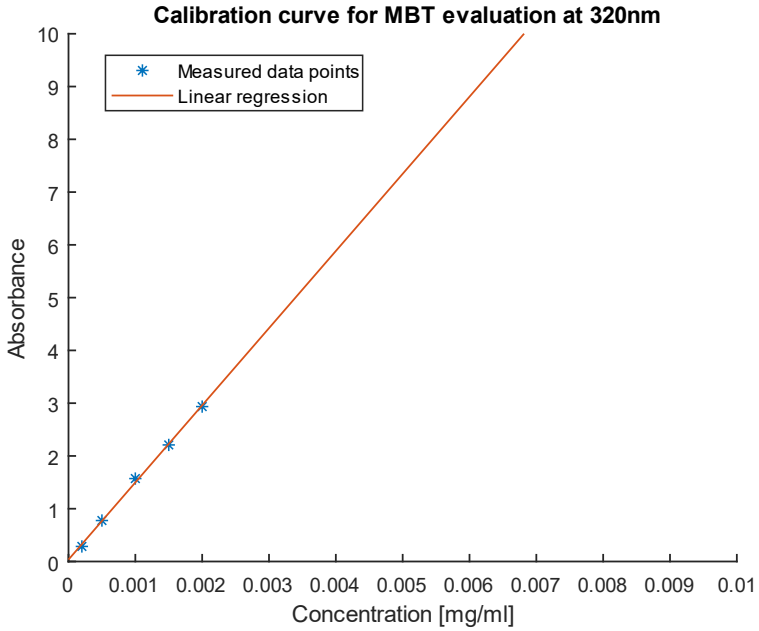

Fig 13b, Calibration curve for MBT

4.3 SURFACE PROPERTIES

The results of the coating depth test and the contact angle of water on the coating is presented in table 2 and 3, respectively. Microscopic pictures taken of the surface distribution of all the different iteration of the coatings made are presented in fig 14-24. In the iterations with pollen in the coating in fig 14-20, the darker parts present are the pollen spores. In the iterations without any pollen or crosslinked with GA, fig 21-23, the darker parts are air bubbles entrapped in the coatings. In fig 24 no bubbles were formed, and the darker areas are impurities such as dust particles.

Coating *thickness*

Table 2, coating thickness of samples applied to stainless-steel plate by pipette.

Coating	25DS	50DS	100DS	25DS-7GA	50DS-4GA	50DS-7GA	50DS-10GA	25DS-X	50DS-X	100DS-X	25DS-7GA-X
Thickness [μm]	83	37	62	93	56	66	41	25	32	30	26

Contact angle

Table 3, contact angle of water droplet applied to the coatings.

Coating	25DS	50DS	100DS	25DS-7GA	50DS-4GA	50DS-7GA	50DS-10GA	25DS-X	50DS-X	100DS-X	25DS-7GA-X
Contact angle	32.5	45.5	37	32	25	17	37	36	44	47	33.5

Surface structure

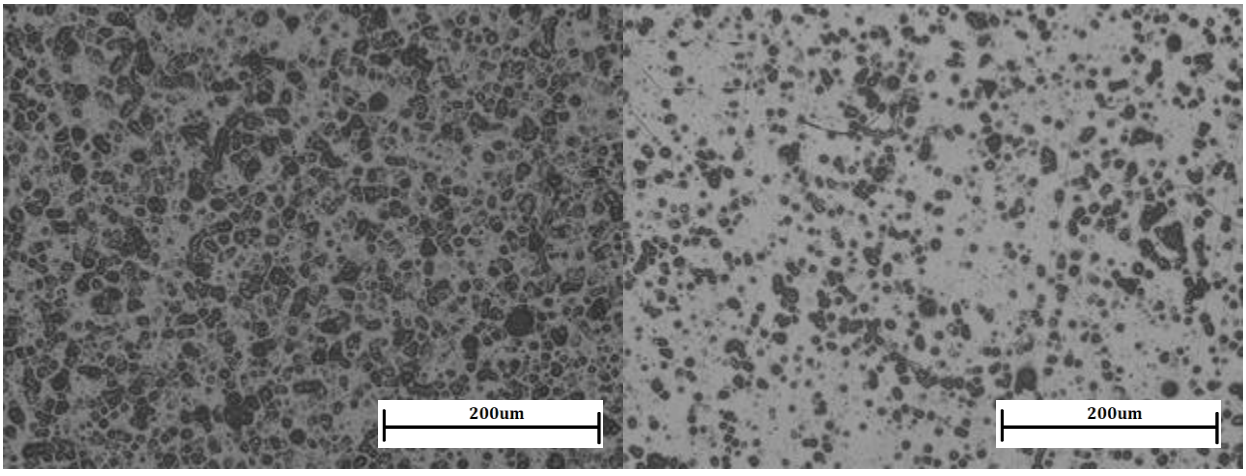

Fig 14, 25DS

Fig 15, 50DS

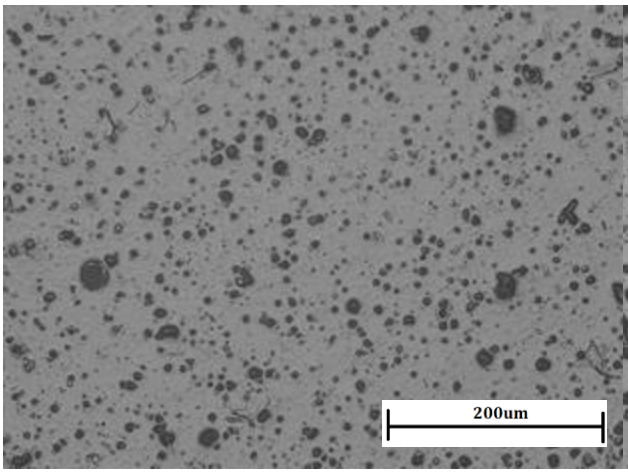

Fig 16, 100DS

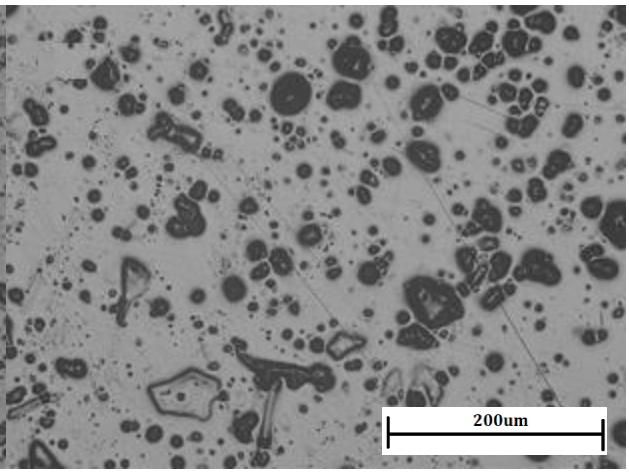

Fig 17, 50DS-4GA

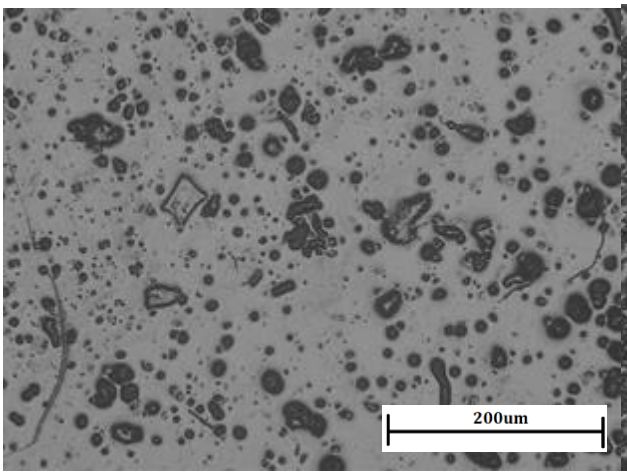

Fig 18, 50DS-7GA

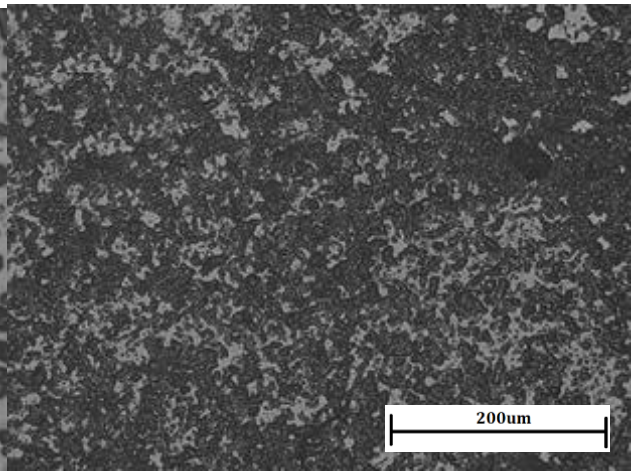

Fig 19, 50DS-10GA

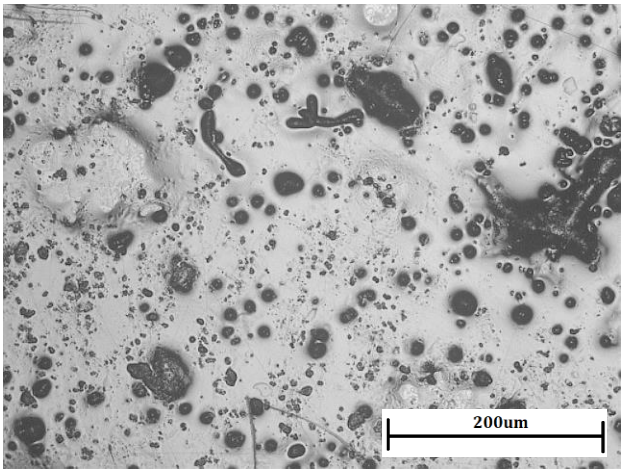

Fig 20, 25DS-7GA

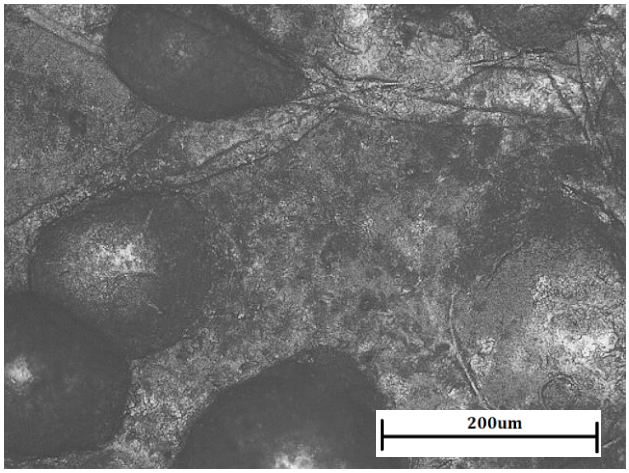

Fig 21, 25DS without pollen

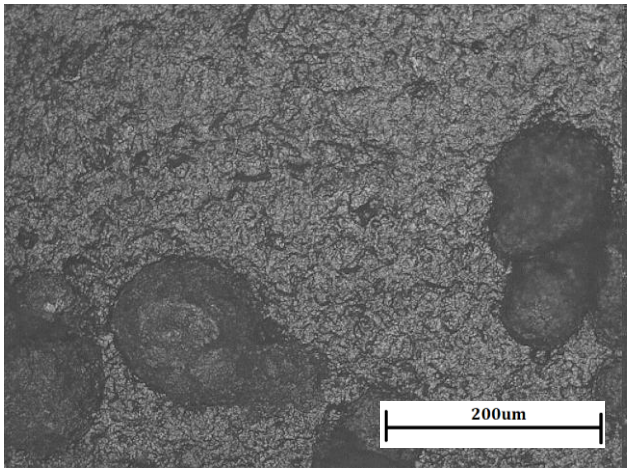

Fig 22, 50DS-X without pollen

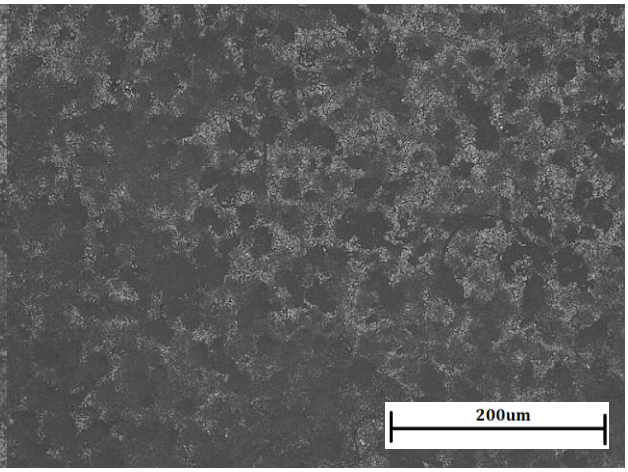

Fig 23, 100DS-X without pollen

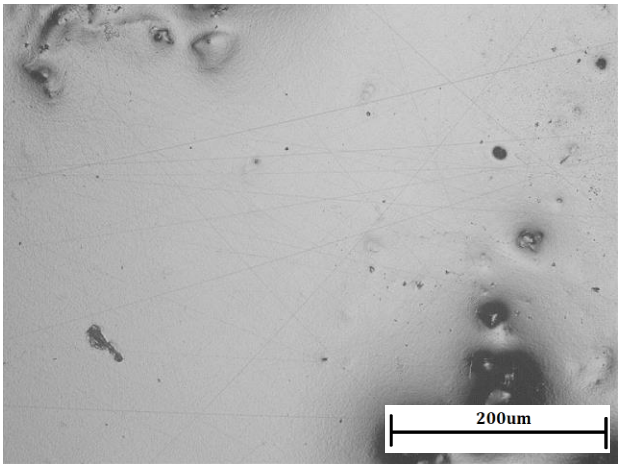

Fig 24, 25DS-7GA-X without pollen

4.4 FTIR OF ISOLATED REACTIONS

The isolated reactions of the different potential reactions between the components of the coating is presented in fig 25- 30.

Pollen-OA and SA reaction

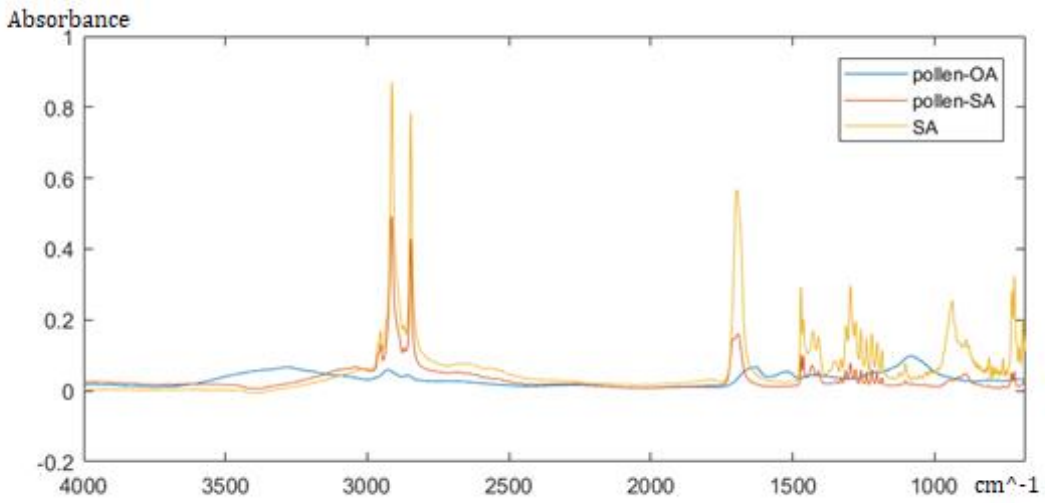

Fig 25, FTIR-ATR absorbance of Pollen-OA and SA reaction.

Pollen-SA and MBT reaction

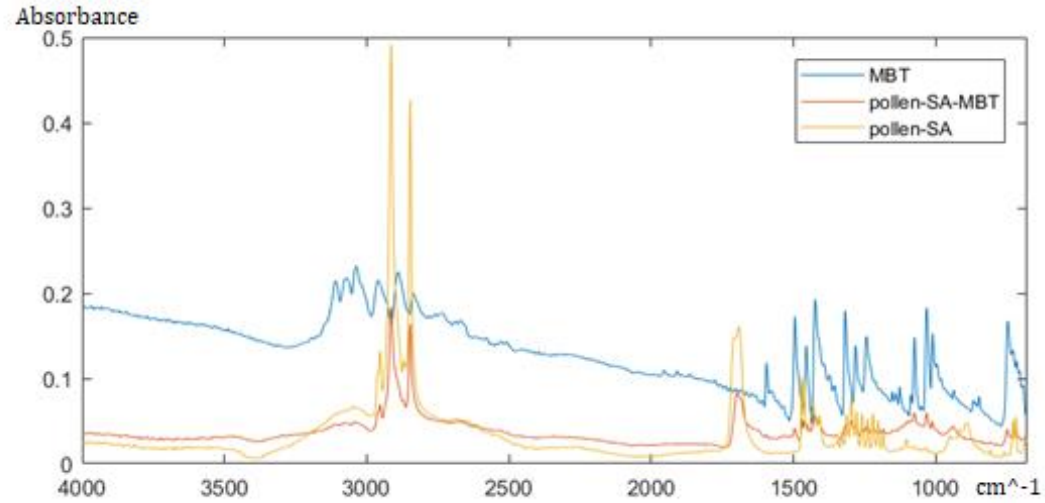

Fig 26, FTIR-ATR absorbance of Pollen-SA and MBT reaction

Pollen-SA-MBT-CS and GA reaction

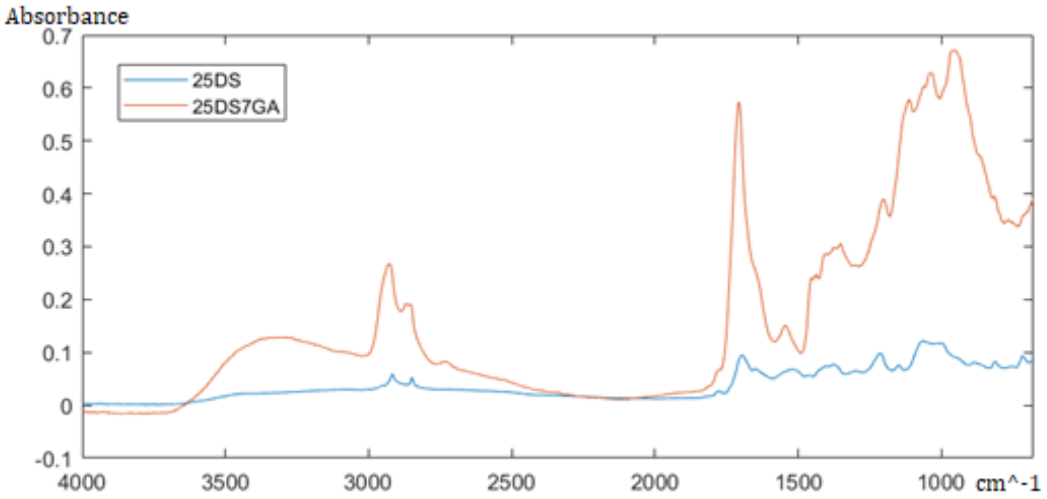

Fig 27, FTIR-ATR absorbance of Pollen-SA-MBT-CS and GA reaction

Pollen-OA and CS reaction

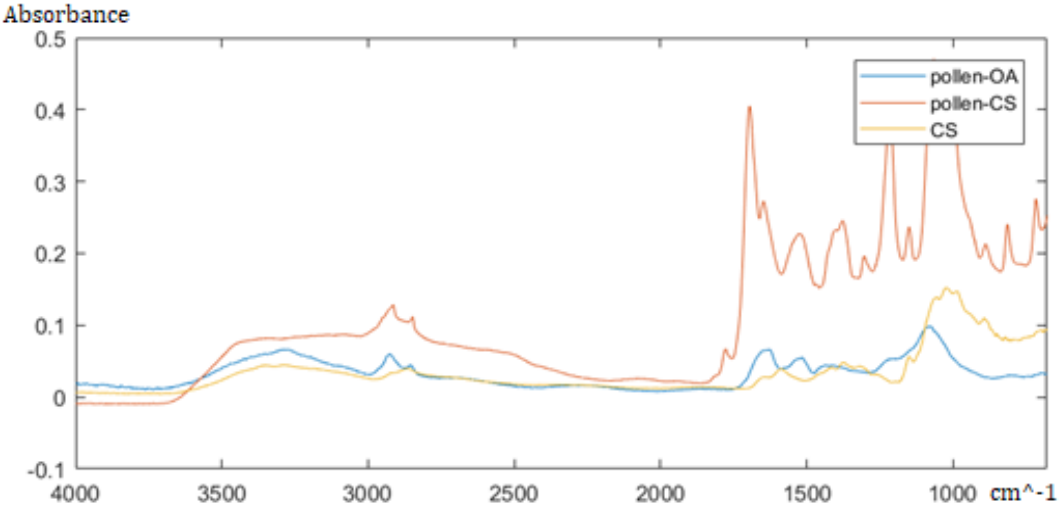

Fig 28, FTIR-ATR absorbance of Pollen-OA and CS reaction

Pollen-OA and MBT reaction

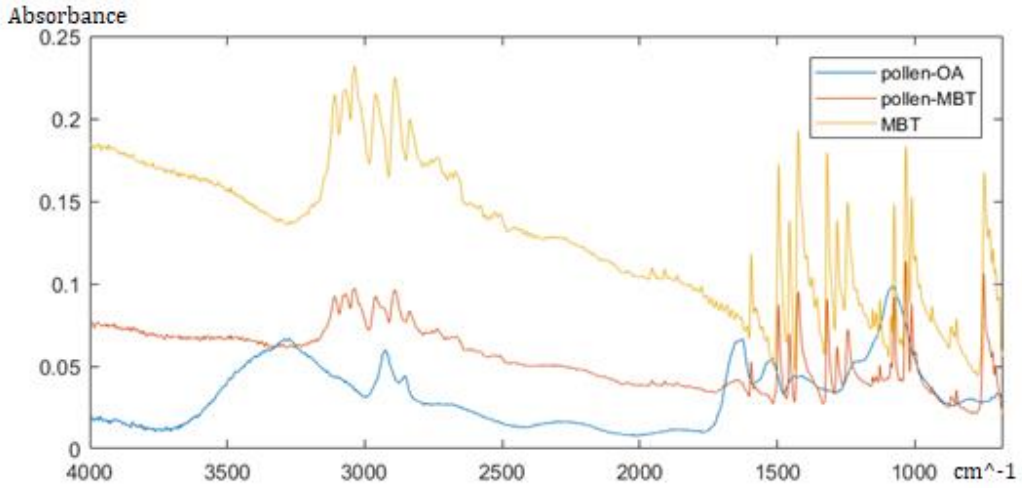

Fig 29, FTIR-ATR absorbance of Pollen-OA and MBT reaction

Pollen OA and GA reaction

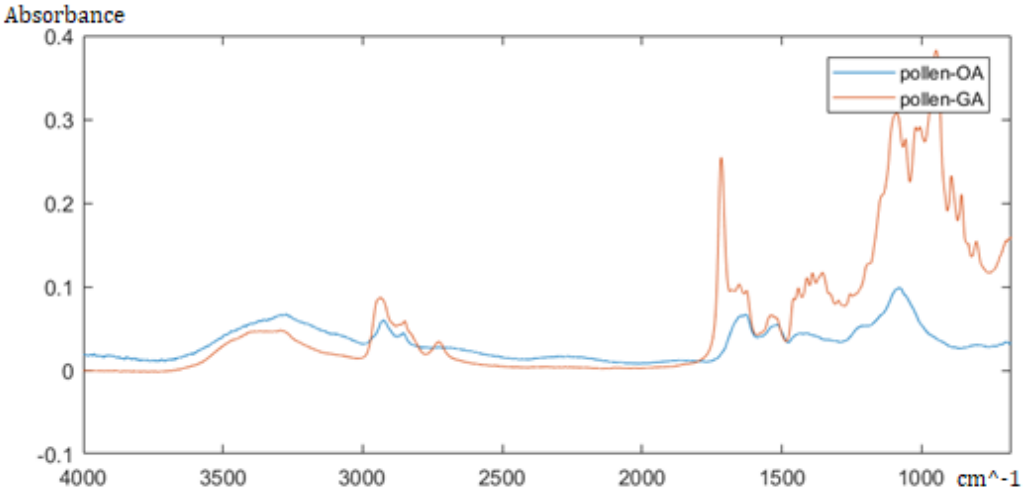

Fig 30, FTIR-ATR absorbance of Pollen-OA and GA reaction

4.5 SUBMERSION TEST

The results of the submersion tests, where coated plates had been submerges in water is presented in fig 31-40.

The 50-7 coating in fig 31 remained intact and attached to the surface. No bubbles were formed under the coating. The edges of the coating got a whitish hue as it was submerged. After drying the coating cracked up completely and detached from the surface. The top of the flakes still had its golden color while the side that was against the surface got a pure white color.

The 50-4 coating in fig 32 remained intact and attached to the surface. Small bubbles formed in between the coating and the surface. The edges of the coating got a whitish hue as it was submerged. After drying cracks were formed where the bubbles had formed.

The 25-7 coating in fig 33 formed wrinkles on its surface as it was applied to the steel plate. The coating remained intact and attached to the surface and no bubbles were formed under the coating. As the coating dried it cracked up completely and detached from the surface. The flakes were homogeneous.

The 50-10 coating in fig 34 remained attached to the surface, although bubbles formed in between the coating and the surface. The top of the coating also gelated and were easily removed.

The 25DS coating in fig 35 remained mostly intact and attached to the surface. Bubbles were formed under the coating. As the coating dried it partially detached from the surface and some cracks were formed were the bubbles were formed.

The 50DS and 100DS coatings dissolved into strings and small sheets of a few mm length. The 50DS were more prone to form sheets, while the 100DS formed strings with connected agglomerations, as seen in fig 36.

The 25DS-X coating in fig 37 was detached from the surface as a single sheet, and after removed from the water it had swelled at least 10 times in size and formed a gel. The red color is a discoloring from a marker and did not affect the result any.

The 50DS-X coating in fig 38 was partially detached from the surface but remained intact and did not dissolve any.

The 100DS-X coating in fig 39 was dissolved partially and small pieces floated to the surface of the water.

The 25DS-7GA-X coating in fig 40 turned into a whitish color as it was submerged, from its more golden color it had before. As it dried, the coating mitigated from the edges, and no cracks was present.

Note that some circular indents from the FTIR such as seen in fig 35 and 38, and scratches from testing the strength of the coatings as seen in fig 40 are present. These have been determined to not affect the tests, as they did not solely act as the initiation points of the observed results.

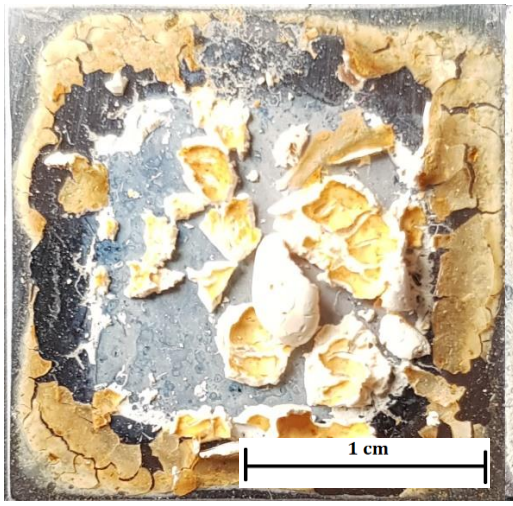

Fig 31, 50DS-7GA after submersion

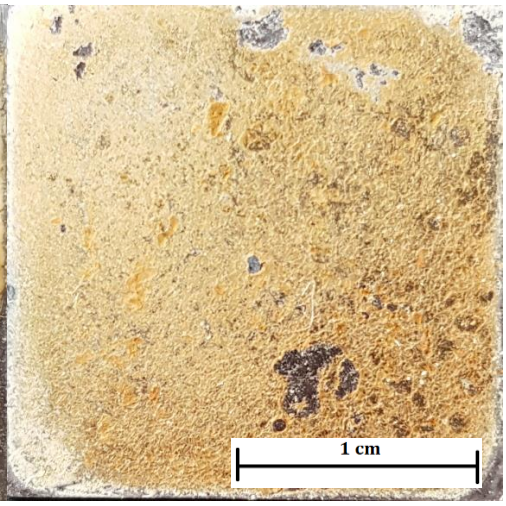

Fig 32, 50DS-4GA after submersion

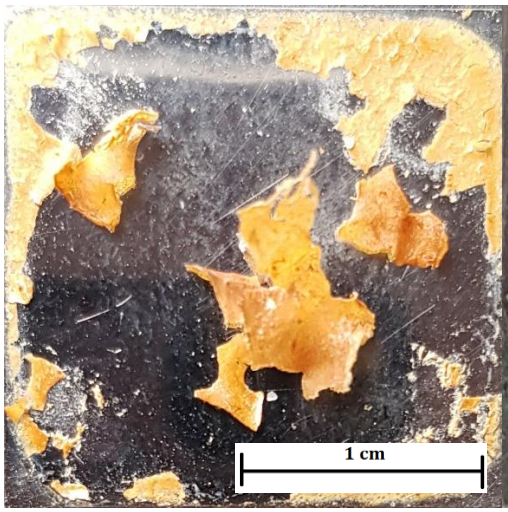

Fig 33, 25DS-7GA after submersion

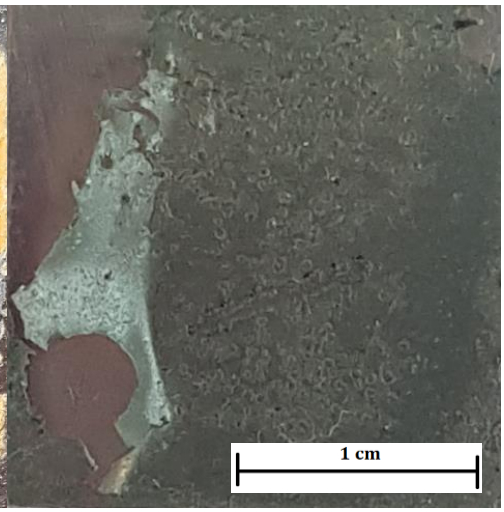

Fig 34, 25DS after submersion

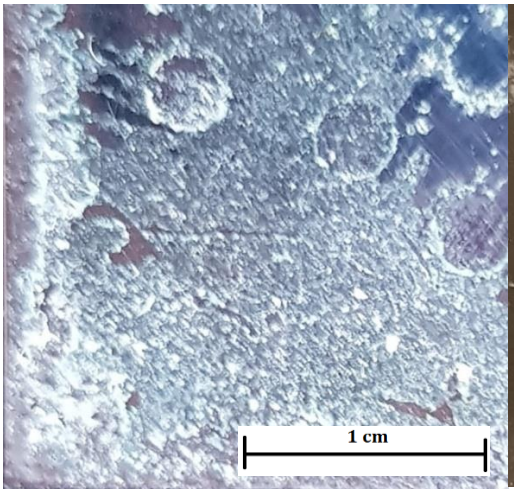

Fig 35, 50DS-10GA after submersion

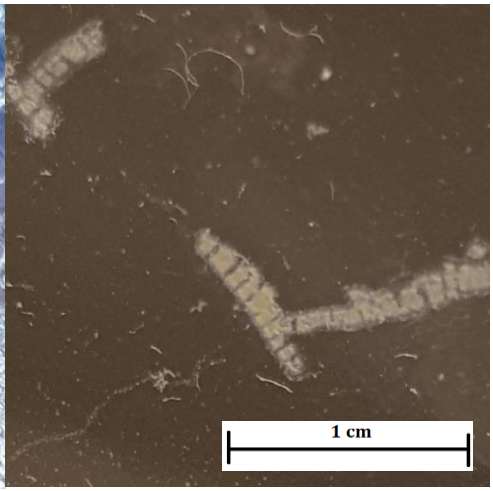

Fig 36, 100DS dissolved in water

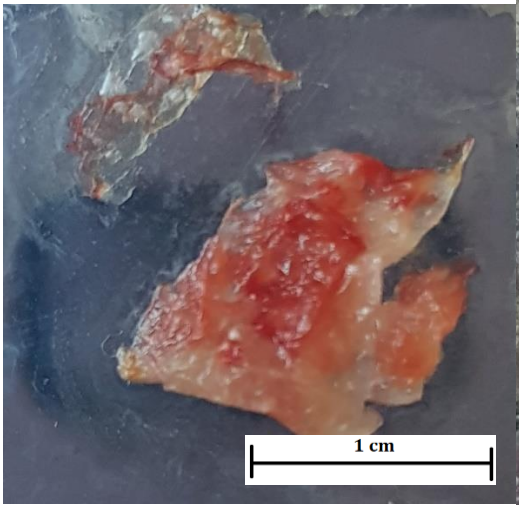

Fig 37, 25DS-X after submersion

Fig 38, 50DS-X after submersion

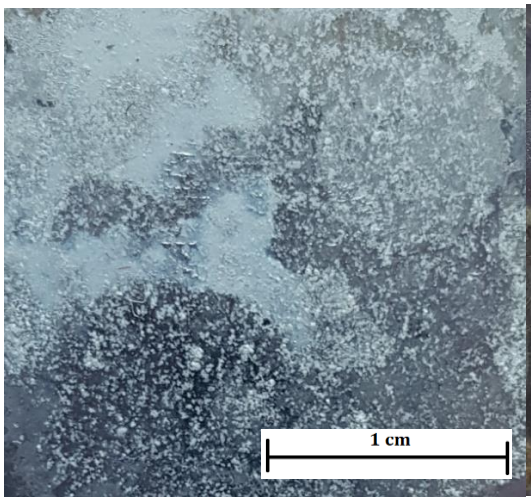

Fig 39, 100DS-X after submersion

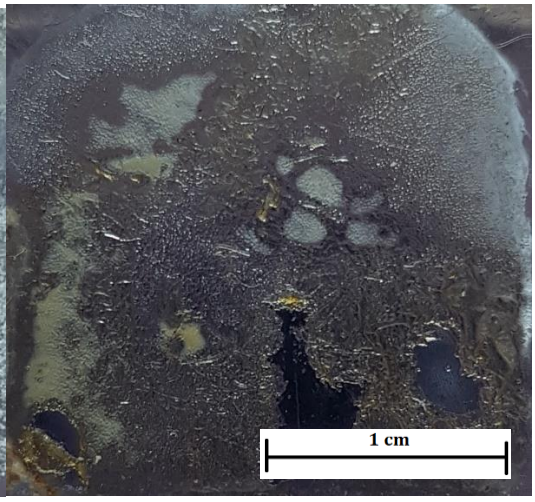

Fig 40, 25DS-7GA-X after submersion

5 DISCUSSION

5.1 DEGREE OF DEACETYLATION OF CHITOSAN

The curves achieved in fig 10a were similar as those found in the literature as seen in fig 8 confirming that our calibration curve is to be reliable. The DDA of commercial chitosan was determined to be at 88.5% which is higher than what we first expected, as generally the DDA of commercial chitosan are usually not as high. After treatment the chitosan achieved a DDA of 91.5%, which was an improvement although as the process of washing the chitosan after the deacetylation is quite tedious to do and the improvement was not that great, a decision was made that the DDA of the commercial chitosan is sufficient, and was to be used in this rest of the study.

5.2 FORMULATION OF CHITOSAN-STEARIC ACID COATING

5.2.1 chitosan-stearic acid crosslinking

The EDC/NHS crosslinking provide a binding as shown in fig 7, where (1) is the SA and (2) is the CS. This will prove an increase of the primary amide bond C=O whose absorbance will increase if an increased amount of those bonds is found in the analyzed powder, whose bonds will be shown at 1690 cm^{-1}, and also a reduction of the N-H bond, found at the 3200 cm^{-1} range. In fig 11, a clear reduction around 3200 cm^{-1} and an increase at 1690 cm^{-1} provide an indication that crosslinking is done in the CS-SA polymer.

5.2.2 Loading pollen into chitosan-stearic acid

Iteration 1 – adding pollen into formed micelles

As the pollen precipitated as quickly as they did the pollen did most likely not get encapsulated into the micelles nor formed a stable solution. CS-SA micelles are according to literature a lot smaller than the pollen spores, which could indicate that they simply did not fit into the micelles and therefor was left outside.

Iteration 2 - 50DS, pollen added before forming micelles

A homogeneous solution was formed which were opaque and foamy, probably due to an excess amount of unreacted SA remaining in the solution. Washing the solution by centrifugation and decanting prior to crosslinking it with chitosan to remove any unreacted SA would be to be preferred to reduce the foaming as well as achieving a clearer product. After a few hours, a very small amount of pollen was seen precipitated on the bottom in form of a brownish slur. This is determined to not be a problem, as it still is stable for a long enough time after stirring that it should be no problem to apply it on a surface and achieve a homogeneous distribution of the pollen.

Iteration 3 – 25DS, pollen added before forming micelles

A homogeneous solution was formed which were clear and without foam, which could confirm that the foam in the previous iteration was due to the unreacted SA, and also confirms that the washing is a desired step. Same as the previous iteration a small amount of pollen was seen precipitated on the bottom after a few hours.

5.2.3 Loading 2-mercatzobenzothiazole into chitosan-stearic acid

The amount of loaded MBT in the pollen in the CS-SA were consistent over different dilutions as seen in table 1. The average LC of MBT in CS-SA is about 0.75%, which although being on the lower end of what is wanted, it is determined to be sufficient. As the pollen core might not have been thoroughly cleaned as it was only washed thrice while in previous studies [23] it had been done up to 14 times, it could cause less MBT to be able to be encapsulated. The less thorough washing was done due to it was determined it is only needed to be that clean while being used for drug delivery.

5.3 SURFACE PROPERTIES

Coating thickness

The thicknesses of the coatings were in the 40-80μm range as seen in table 2, besides the iterations without pollen, 25DS-X, 50-DSX, 100-DSX and 25DS-7GA-X which were a bit lower. Each layer of application added about 15μm thickness.

An initial attempt to apply using an air brush was used as that is what would be used commercially for application of the coating. The thickness of each applied layer was though only about 4μm, and the airbrush was needed to be cleaned between each application made it too tedious, as well as giving a similar result as to application by pipette.

Contact angle

The contact angles as seen in table 3 were reduced when crosslinked with the GA, which were not to be expected as the extra crosslinking should have made it more hydrophobic by reducing the amount of amine groups. While looking at the iterations without pollen, 25DS-X, 50DS-X and 100DS-X, it appears that the hydrophobic nature of the coating increases as the DS goes up, although when then further crosslinked with GA in the 25DS-7GA-X iterations, the hydrophobicity lowers again.

Surface distribution

The surface distribution looks homogeneous throughout all the coatings. A main difference between the coatings only crosslinked with SA and the ones further crosslinked with GA is an increased agglomeration of the darker particles, which is the pollen, particularly in the iterations with a higher amount of GA.

In the iterations without pollen fig 37-39, large bubbles were formed while the coating dried, which appear as dark circles in the figures, and the size of the bubbles were decreased as the DS went up. As the micelle sizes also decreases with increased DS, a cause of the bubble could be that the micelles have entrapped some gas while suspended in the solution, which was kept entrapped even after the coating dried.

5.4 FTIR OF ISOLATED REACTIONS

Pollen-MBT and pollen-SA-MBT

No apparent reactions seem to take place with the MBT, as no new clear peaks were formed in fig 26 and 29.

Pollen-SA

The OA on the pollen is bound to the pollen with the COOH head,

Since the only difference between OA and SA is a double conjugate bond of C atoms on the OA, the only difference between pollen-OA and pollen-SA is a reduced peak at 950 cm^{-1} and 1650 cm^{-1} which corresponds to the bending and stretching of the bonds, which is apparent in fig 25. This could indicate that the SA has successfully attached to the pollen and the OA washed away.

Pollen-CS

Looking at the EDC in fig 7 which has an N=C=N bond with a peak at 2130cm^{-1} which can not be found in the spectra in fig 28, which would indicate that the EDC has been spent, and crosslinking has taken place. New peaks at 1210 cm^{-1} and 1300 cm^{-1} which corresponds to the C-N formation as well as a removed peak at 3300 cm^{-1} which corresponds to the N-H bond removed confirms a crosslinking of a carboxyl and amine.

A new broad peak at 3300-2500 cm^{-1} corresponds to the O-H stretching as well as peaks at 1700 cm^{-1} and 1780 cm^{-1} related to the C=O stretching of carboxylic acid which could indicate that the oleic acid has detached from the pollen surface.

Additional new peaks at 1210 cm^{-1}, 1300 cm^{-1} and 1650 cm^{-1} can be seen which could indicate the presence of isourea and NHS remaining in the solution as byproducts of the EDC/NHS reaction. These products also have C-N and N-H bonds that is relevant to the crosslinking, although these substances are estimated to be low enough to now interfere.

Pollen-GA

No too apparent new peaks have formed as seen in fig 30, which would indicate that no reaction has taken place between the GA and the pollen.

Pollen-SA-MBT-CS + GA

The crosslinking between CS and GA is made by forming an imine bone, which has a peak at 1690 cm^{-1}, which unfortunately is also where the peak of C=O of GA is at. The imine bond is formed by the primary amine, with peaks at 1600 cm^{-1} and 3450cm^{-1}. At 3450cm^{-1} in fig 27, the GA has a peak related to the O-H stretching which interferes with the interpretation. At 1600 cm^{-1} an inversed peak is shown, which shows that the crosslinking is effective.

5.5 SUBMERSION TEST

The complete dissolvement of the 50DS and 100DS coatings as seen in fig 36 could be because the micelle size is reduced with increased crosslinking, causing the micelles to form outside of the pollen or just simply not forming a covering surface around it. It could also be that the micelles are the cause of the dissolvement, as it might cause less or no crosslinking across the different pollen grains, and instead only form polymers locally at the pollen, which in turn gives the polymer a low strength to stick together on the macroscopic scale. This could be an indication of the connected agglomerations of the chain as seen in fig 36, and instead of the micelles forming around the pollen, it forms micelles that cover the surface of the pollens.

Besides the 25DS-7GA coating, bubbles were formed under the coatings which caused severe damage to the coating after drying. This could be because the coatings are too hydrophilic and absorbs to much water and passing through possibly to the pollen to form these bubbles. The 25DS-7GA coating could have a proper network structure to make it so the water does not reach the pollen to form theses bubbles. This could also be a reason to the slow drying of the coating when first applied, as the network reduced the mobility of water and hence makes it unable to diffuse and vaporize as quickly. The lower DS might be too low to properly form micelles which could further increase the network structure.

The gelation of 25DS in fig 34 could possibly be because the polymer gets to mobile while in water, making the shorter polymers get partially untangled and float up. The increased gelation of the top of the coating could be explained if the gelation is increased with lower molecular weight.

The change in homogeneity of the 50DS-7GA coating could be in a similar fashion, where the white part (possibly SA-heavy) remained on the bottom while the golden part (possibly pollen and/or GA heavy) have a lower density and thanks to the increased mobility in water gets shifted to the top. The destructive cracking caused while the coating dried could be due to the expansion while in water is different from the white and golden sides, causing high tensions to be created when dried. The flakes had a convex curvature with golden side on the inside, which would indicate that this part retracted more while dried. The Marangoni effect could be the cause of this, which would also explain the whitening of the edges of the 50DS-7GA and 50DS-4GA coatings.

The 25DS-X, 50DS-X, and 100DS-X coatings in fig 37-39 show that the optimal DS for a CS-SA coating is in the middle ranges. As the DS goes lower as in 25DS-X the film forming properties of chitosan is heavily favored, as the whole coating came off in a single piece, although it swelled way too much in the water. As the DS goes up the micelle formation become more prominent, although this reduces the strength of the coating to such a degree that a slight shaking of the beaker causes the coating to come off.

As the 25DS-7GA-X coating in fig 40 did not show any cracks, only some wringed caused by the evaporation of the absorbed water in the coating, shows that the pollen is much likely the cause of the violent cracking of the other of the GA crosslinked iterations.

The whitening of the GA crosslinked iterations shows the possibility that the GA replaces the SA from the chitosan, causing SA to be loose. As then the coatings start to swell in the water, the SA remains in its place as the rest of the coatings clumps up to the center of the plates, leaving a string of white SA on the edges. If this interaction is taking place, the idea of further crosslinking the CS-SA with GA would not be possible without the use of some other crosslinker, if at all.

Overall, the coatings are more brittle after being submerged, hence the tendency for fracture. Besides the most likable cause of the pollen grains just being too big, one possibility could be that as the coatings are submerged some particles, possibly the byproducts of the EDC/NHS reaction, that were unbounded to the polymer but in the solvent worked as a lubricant to make the coating less brittle. These additives were then washed away as the coating was submerged, making the coatings more brittle without them. Another possibility would be that some reaction has taken place while in the water, however it is unsure as of what it could be, as there already was water in the solvent. A third possibility could be that as the polymer swells in the water the polymers gets more mobile, which may cause the chains to entangle in a way that causes high amount of tension to make it crack.

5.6 SOCIAL AND ETHICAL ASPECTS

This coating is an approach to contribute to a reduction of released toxins and undegradable microplastics into the environment and the oceans. By using only and biocompatible chemicals in the process, even if the coating were to be left in the environment for a prolonged time it would not cause any hard, contrast to the more commonly coatings made from epoxy or polyurethane, and if consumed by any animal it would naturally decompose as chitosan is an amino sugar. Neither will any chemicals that affect the wildlife will be used, in contrast to for instance the commonly used heavy metals in commercial coatings.

The main components, chitosan and bee pollen are products from animal agriculture, where chitosan is made from the byproduct of shellfish and bee pollen are taken from beehives that would have been used as food for the bee's larvae. Depending on whom one might ask if it is ethical to use such products for a coating different answers will be provided. The mean man would most likely say it is only a god thing to fully optimize the use of animal byproducts, while the more devoted animal rights activists might say it doesn't matter that it's for the benefit of the environment.

6 CONCLUSIONS AND FURTHER WORK

6.1 CONCLUSIONS

Corrosion protection

The niche of this project was mainly two things: to incorporate the pollen grains as microcapsules for encapsulation of MBT, and the use of CS-SA micelles for the matrix and for further encapsulation effect, and use this as an anti-corrosion coating with a prolonged release of MBT along with self-healing properties for use in aqueous environments. A most basic criteria for such a coating to be efficient is that the coating acts as a barrier with a non-porous layer, to avoid any electrolytes to reach the surface below. None of the iterations done in this project managed to keep that up for more than a short while as it was submerged in water. The best iterations for this was the 25DS-7GA and 50DS-7GA as they remained in the water, although as these was moved from the water they cracked violently. All the coatings had too much of a hydrophilic nature, causing them to not achieve a proper barrier against water, and even though there are uses of hydrophilic coatings, they would be no good for corrosion protection as the electrolytes will penetrate the coating. So as the barrier protection of the coatings was incomplete, no tests of how well the pollen's and MBT 's effect is on the corrosion protection was made.

Pollen as a microcapsule

Pollen has a very complex structure which give the possibility of unknown and unwanted reactions to take place. For one, any attempts to try and increase the hydrophobicity turned out to give the reverse effect than that of when pollen was left out, which most likely is due to the pollen and chitosan gets crosslinked in unwanted ways during the EDC/NHS reactions. Another, and possibly the most critical problem with pollen is its relatively massive size compared to the rest of the system, which causes problem with the micelle formation as well as causing cracking of the GA crosslinked systems.

Crosslinking

The crosslinking with GA is a great way to achieve additional self-healing properties and to improve the strength of chitosan coatings. Apparently, the problem arises when SA is in the picture, as it would appear that the SA gets removed from the chitosan and leave it loose in the solution, completely nullifying the effect of having SA in the beginning, as well as giving us no control over the tuning of amide groups left on the chitosan.

MBT loading

The loading of the MBT into the pollen was successfully done, although due to the lack of barrier properties of the coating no actual tests on the efficiency of its corrosion protection was able to be done, and besides a decent Loading Capacity of MBT in chitosan no results on the corrosion protection can be reported. Using a different matrix than chitosan could most likely be used to evaluate this, or maybe even a different chitosan derivative that does not incorporate micelles, which due to the different in size to pollen causes issues. If one is set to use a CS-SA micelle matrix, a new capsule needs to be used which most likely must be in the nano scale to better fit the sizes of the micelles.

Surface attachment

The attachment of the coatings onto the steel plates were good when the coating was further crosslinked using GA, but for those that were not the coating tended to more or less detach from the plates. The initiation of this detachment was caused due to water penetrated the coating. It is common for coatings to use a primer to improve the attachment strength of the main coating, which could possibly remove this problem for the equation. Although as the coatings water absorption is quite high the primer in itself has to withstand the water as well.

Application method

Initially the application of the coating was used with spray coating as this is was would be most efficient to be used on larger surfaces on a commercial scale, although the application was proven to be too tedious as dozens of layers was needed to achieve a proper coating depth. Instead application was made by adding a droplet on the surface, and no apparent differences of the two application techniques was witnessed. More advanced application methods such as layer-by-layer deposition was not considered as this would make the application to complex as well as impossible to apply without advanced equipment.

6.2 FURTHER WORK

As there seems to be multiple issues that cause the coatings created to fail, mainly being the reactivity and size of the pollen, the idea to incorporate pollen as a microcontainer in a CS-SA matrix is unsuccessful. If one wants to use the CS-SA matrix, it could be wise to experiment with using capsules on the nanoscale instead of the microscale that pollen is in, such as carbon nanotubes to encapsulate MBT.

Due to the covid-19 situation, many planed experiments were not made, which could provide useful information to give a base for further work. One of such would be to determine the achieved degree of substitution of amides to SA on the chitosan, to provide a better base to determine the effect of the crosslinking degree.

All in all, it would not be recommended to do further attempts to incorporate pollen into an anti-corrosion coating, although the CS-SA matrix could be evaluated more thoroughly as it proved to have potential when tested without the pollen, and testing smaller sized capsules for the encapsulation. It could also be of interest to test how different crosslinkers would respond to the reactivity of the pollen.

7 REFERENCES

[1] American Coatings Association, Environmental Impact, https://www.paint.org/about/industry/environmental-impact/ (Accessed: 21 Feb 2020)

[2] Wikipedia, Environmental impact of paint, https://en.wikipedia.org/wiki/Environmental_impact_of_paint (accessed: 21 Feb 2020)

[3] Qi Bao et al., 2-Mercaptobenzothiazole doped chitosan/11-alkanethiolate acid composite coating: Dual function for copper protection, Applied Surface Science, 2011, Available: https://www.sciencedirect.com/science/article/pii/S0169433211010890

[4] Hojat Jafari et al., Corrosion Inhibitor of carbon steel immersed in a 1M HCl solution using benzothiazole derivatives, Arabian Journal of Chemistry, 2019, Available: https://www.sciencedirect.com/science/article/pii/S1878535214002664

[5] Qian Bei et al., Self-Healing Epoxy Coatings Based on Nanocontainers for Corrosion Protection of Mild Steel, Journal of Electrochemical Society 164(2), 2017, C54-C60, Available: https://www.researchgate.net/publication/312258341_Self-Healing_Epoxy_Coatings_Based_on_Nanocontainers_for_Corrosion_Protection_of_Mild_Steel

[6] Yuan Yang et al., Ligand-Directed Stearic Acid Grafted Chitosan Micelles to Increase Therapeutic Efficacy in Hepatic Cancer, molecular pharmaceutics, 2014

[7] Feng Cao, et al., Morphology-controlled synthesis of SiO_2 hollow microspheres using pollen grain as a biotemplate, 2009, Biomedical Materials, Available: https://iopscience.iop.org/article/10.1088/1748-6041/4/2/025009

[8] Alberto Diego-Taboada et al., Hollow Pollen Shells for Enhanced Drug Delivery, 2014, Pharmaceutics 6(1):80-96, Available: https://www.researchgate.net/publication/260875436_Hollow_Pollen_Shells_to_Enhance_Drug_Delivery

[9] Chawla, S.P. et al, "Chitosan" in *Polysaccharides Bioactivity and Biotechnology*, Springer, Switzerland, 2015, ch8, p219-246

[10] Jennings J. Amber et al, Deacetylation Modification Techniques of Chitin and Chitosan, Woodhead Publishings,2017, ch11, p257

[11] Jia-Ru Ye et al., Turning the chitosan surface from hydrophilic to hydrophobic by layer-by-layer electro-assembly, RSC Advances, 2014, available: https://pubs-rsc-org.focus.lib.kth.se/en/content/articlelanding/2014/RA/C4RA10327K#!divAbstract

[12] Yuan H et al., Stearic acid-g-chitosan polymeric micelle for oral drug delivery: in vitro transport and in vivo absorption, Mol Pharm, 2011, Available: https://www.ncbi.nlm.nih.gov/pubmed/21138243

[13] Fu-Qiang Hu et al., A novel chitosan oligosaccharide–stearic acid micelles for gene delivery: Properties and in vitro transfection studies, International Journal of Pharmaceutics, 2006

[14] Wikipedia.org, Kraft Temperature, https://en.wikipedia.org/wiki/Krafft_temperature (accessed: 20 Apr 2020)

[15] Wikipedia.org, Mercaptobenzothiazole, https://en.wikipedia.org/wiki/Mercaptobenzothiazole (accessed 21 Jan 2020)

[16] Tiago L.P Galvão et al., A computational UV–Vis spectroscopic study of the chemical speciation of 2-mercaptobenzothiazole corrosion inhibitor in aqueous solution, 2016, Available: https://link.springer.com/article/10.1007/s00214-016-1839-3

[17] Yuanyuan Feng et al., Characterization of iron surface modified by 2-mercaptobenzothiazole self-assembled monolayers, Applied Surface Science, 2006, Available: https://www-sciencedirect-com.focus.lib.kth.se/science/article/pii/S0169433206007720#bib2

[18] Jennings, G.K et al., Structural effects on the barrier properties of self-assembled monolayers formed from long-chain ω-alkoxy-n-alkanethiols on copper, Journal of American Chemical Society, 2003, Available: https://www.scopus.com/record/display.uri?eid=2-s2.0-0037433556&origin=inward&txGid=080b4855726572d0a5ec9756eed1cf52

[19] Frederico Maria et al., Silica nanocontainers for active corrosion protection, Nanoscale, 2012, Available: https://pubs-rsc-org.focus.lib.kth.se/en/content/articlelanding/2012/NR/c2nr11536k#!divAbstract

[20] Ying-Hsuan Chen et al., The multiple roles of an organic corrosion inhibitor on copper investigated by a combination of electrochemistry-coupled optical in situ spectroscopies, Corrosion Science, 2018, available: https://www-sciencedirect-com.focus.lib.kth.se/science/article/pii/S0010938X17320012

[21] Xia, Y., et al., *Biotemplated fabrication of hierarchically porous NiO/C composite from lotus pollen grains for lithium-ion batteries.* Journal of Materials Chemistry, 2012

[22] Gubbuk, I.H., Gürfidan, L., Erdemir, S. et al. Surface Modification of Sporopollenin with Calixarene Derivative. Water Air Soil Pollut 223, 2623–2632 (2012). Available: https://doi-org.focus.lib.kth.se/10.1007/s11270-011-1054-8

[23] Idris Sargin et al., Chitosan/sporopollenin microcapsules: Preparation, characterisation and application in heavy metal removal, 2015, International Journal of Biological Macromolecules, Available:

https://www-sciencedirect-com.focus.lib.kth.se/science/article/pii/S0141813015000501

[24] Aysel Cimen, Adsorptive removal of Co(II), Ni(II), and Cu(II) ions from aqueous media using chemically modified sporopollenin of Lycopodium clavatum as novel biosorbent, Desalination and water treatment, 2014, available: https://www.researchgate.net/publication/264901419_Adsorptive_removal_of_CoII_NiII_and_CuII_ions_from_aqueous_media_using_chemically_modified_sporopollenin_of_Lycopodium_clavatum_as_novel_biosorbent

[25] Surface Technology, The three types of anti-corrosion coatings explained, http://www.surfacetechnology.co.uk/blog-18-the-three-types-of-anti-corrosion-coatings-explained/ (accessed 21 Jan 2020)

[26] Thomas Industrial Coatings, Three modes of corrosion protection, https://www.thomasindcoatings.com/three-modes-corrosion-protection/ (accessed 17 Apr 2020)

[27] American Coatings Association, Optimum viscosity of paint application, https://www.paint.org/article/optimum-viscosity-paint-application/, (accessed 21 Jan 2020)

[28] Chemistry LibreTexts,Hydrophobic interactions, https://chem.libretexts.org/Bookshelves/Physical_and_Theoretical_Chemistry_Textbook_Maps/Supplemental_Modules_(Physical_and_Theoretical_Chemistry)/Physical_Properties_of_Matter/Atomic_and_Molecular_Properties/Intermolecular_Forces/Hydrophobic_Interactions (accessed 17 Apr 2020)

[29] Syed Taqvi & Ghada Bassioni, Understanding Wettability through Zeta Potential Measurements, Open access, 2019, available: https://www.researchgate.net/publication/333326525_Understanding_Wettability_through_Zeta_Potential_Measurements

[30] R Cade, Surface Tension as a Double-layer Phenomenon, 1963, Proc. Phys. Soc. 82 216, available: https://iopscience-iop-org.focus.lib.kth.se/article/10.1088/0370-1328/82/2/308/pdf

[31] Wikipedia, Double layer (surface science), https://en.wikipedia.org/wiki/Double_layer_(surface_science) (accessed 17 Apr 2020)

[32] AcuWet, AcuWet - Hydrophilic Coating Technology, https://www.youtube.com/watch?v=PqTiEAIboqo, (accessed 17 Apr 2020)

[33] Jing Fu et al., The chitosan hydrogels: from structure to function, New Journal of Chemistry, 2018, Available: https://pubs-rsc-org.focus.lib.kth.se/en/content/articlelanding/2018/NJ/C8NJ03482F#!divAbstract

[34] Fan Zhuang et al., Self-healing mechanisms in smart protective coatings: A review, Corrosion Science, 2018, Available: https://www.sciencedirect.com/science/article/pii/S0010938X17322308?via%3Dihub

[35] Weikang Hu et al., Advances in crosslinking strategies of biomedical hydrogels, Biomaterial Science, 2019, Available: https://pubs-rsc-org.focus.lib.kth.se/en/content/articlelanding/2019/BM/C8BM01246F#!divAbstract

[36] Jiaoyu Ren et al., Highly transparent and self-healing films based on the dynamic Schiff base linkage, RSC Advances, 2016, Available: https://pubs.rsc.org/en/content/articlelanding/2016/RA/C6RA23886F#!divAbstract

[37] Shirish Hari Sonawane et al., Encapsulation of Active Molecules and Their Delivery System, Elsevier, 2020, isbn 9780128193648

[38] Yan Voloshin et al., The Encapsulation Phenomenon, Springer, 2016, Switzerland, ISBN: 978-3-319-27738-7

[39] Frederico Maia et al., Silica nanocontainers for active corrosion protection, https://pubs.rsc.org/en/content/articlelanding/2012/nr/c2nr11536k#!divAbstract

[40] Maria A. Azevado et al., Alginate/chitosan nanoparticles for encapsulation and controlled release of vitamin B_2 , International Journal of Biological Macromolecules, 2014, Available: https://www.sciencedirect.com/science/article/pii/S0141813014003328

[41] Giovanna Rasso et al., Composite chitosan/alginate hydrogel for controlled release of deferoxamine: A system to potentially treat iron dysregulation diseases, Carbohydrate Polymers, 2016, Available: https://www.researchgate.net/publication/283256946_Composite_chitosanalginate_hydrogel_for_controlled_release_of_deferoxamine_A_system_to_potentially_treat_iron_dysregulation_diseases

[42] Jorge Carneiro et al., Chitosan as a Smart Coating for Controlled Release of Corrosion Inhibitor 2-Mercaptobenzothiazole, ECS Electrochemistry Letters 2(6), 2013, Available: https://www.researchgate.net/publication/236694021_Chitosan_as_a_Smart_Coating_for_Controlled_Release_of_Corrosion_Inhibitor_2-Mercaptobenzothiazole

[43] Zhaoying Ding, Smart release of corrosion inhibitors by a novel encapsulation method, M.S. thesis, Faculty of Mech., Maritime and Materials Eng., Delft University of Technology, Netherlands, 2016, Available: https://pdfs.semanticscholar.org/ba2d/05a14ebf27abd6ee30dc1032860d2be22382.pdf

[44] MedLab Pharma, Inc., Nano-Encapsulation, http://www.medlabpharma.com/our-services/nano-encapsulation/ (accessed 17 Apr 2020)

[45] Sigma-Aldrich, Drug Delivery FAQs, https://www.sigmaaldrich.com/technical-documents/articles/materials-science/drug-delivery/drug-delivery-questions.html (accessed 17 Apr 2020)

[46] Nazrul Islam et al., Degradability of chitosan micro/nanoparticles for pulmonary drug delivery, Heliyon, 2019, Available: https://www.researchgate.net/publication/333124906_Degradability_of_chitosan_micronanoparticles_for_pulmonary_drug_delivery

[47] Thermo Scientific, *easy molecular bonding, crosslinking technology,* Thermo Fisher Scientific, 2012

[48] Wikipedia, Ultraviolet-visible spectroscopy https://en.wikipedia.org/wiki/Ultraviolet%E2%80%93visible_spectroscopy , (accessed 22 Mar 2020)

[49] Anthony J. Owen, Uses of Derivative Spectroscopy, Agilent Technologies, 1995, Available: https://www.whoi.edu/cms/files/derivative_spectroscopy_59633940_175744.pdf

[50] Jolanta Kumirksa et al., Application of Spectroscopic Methods for Structural Analysis of Chitin and Chitosan, Marine Drugs, 2010, Available:https://www.researchgate.net/publication/44684157_Application_of_Spectroscopic_Methods_for_Structural_Analysis_of_Chitin_and_Chitosan

[51] Jim Clark, 2016, Chemguide.co.uk, The Beer-Lambert Law, https://www.chemguide.co.uk/analysis/uvvisible/beerlambert. html (accessed 22 Mar 2020)

[52] Muzzarelli, R.A.A. and R. Rocchetti, *Determination of the degree of acetylation of chitosans by first derivative ultraviolet spectrophotometry.* Carbohydrate Polymers, 1985

[53] Wikipedia, Fourier-transform infrared spectroscopy, https://en.wikipedia.org/wiki/Fourier-transform_infrared_spectroscopy (accessed 27 mars 2020)

[54] Dr Michael Bradley, Thermo Fisher, FTIR sample handling techniques for attenuated total reflection (ATR), https://www.thermofisher.com/seen/home/industrial/spectroscopy-elemental-isotope-analysis/spectroscopy-elemental-isotope-analysis-learning-center/molecular-spectroscopy-information/ftir-information/ftir-sample-handling-techniques/ftir-sample-handling-techniques-attenuated-total-reflection-atr.html (accessed 27 mars 2020)

TRITA ITM-EX 2020:309